Rev. Ivoir. Sci. Technol., 16 (2010) 11 – 50 11
ISSN 1813-3290

NON-PLANAR CRACK UNDER GENERAL LOADING : DISLOCATION, CRACK-TIP STRESS AND CRACK EXTENSION FORCE

P. N. B. ANONGBA

U.F.R. Sciences des Structures de la Matière et de Technologie, Université de Cocody, 22 BP 582 Abidjan 22, Côte d'Ivoire

(Reçu le 15 Mai 2010, accepté le 07 Septembre 2010)

* Correspondance et tirés à part, e-mail : *anongba@yahoo.fr*

ABSTRACT

This paper investigates the mixed mode I+II+III loading of a non-planar crack fluctuating about an average fracture surface $h = h(x_1)$ that departs from Ox_1x_3 in an infinitely extended isotropic elastic medium. The crack consists of a continuous distribution of three types of non-straight dislocation with infinitesimal Burgers vectors: types 1 and 2 are edges on average and different in nature (1 responding to the mode I loading and 2 to mode II) and type 3 corresponds to screws on average responding to mode III loading. The dislocations are directed along the x_3- direction and spread in x_2x_3- planes in a small oscillating shape $\xi = \xi(x_1, x_3)$ at an average elevation $h(x_1)$. The displacement and stress fields of three dislocations, with arbitrary shape and average character of edge or screw type, are first given. Expressions for the stress about the crack front and crack extension force G per unit length of the crack front are also given. Formula for a spatial average $< G >$ of G is provided for a special crack having a segmented front. Crack configurations for which $< G >$ is larger than the value corresponding to that of a planar crack in Ox_1x_3 under mixed mode I+II+III loading are revealed by the present analysis thus corroborating the occurrence of non-planar fracture abundantly observed in real materials.

Keywords: *Crack propagation and arrest; Energy release rate; Dislocations; Crack mechanics; Energy methods*

RÉSUMÉ

Fissure non plane sous sollicitation extérieure arbitraire : dislocation, contrainte en tête de fissure et force d'extension de la fissure

Cet article étudie la sollicitation, en mode mixte I+II+III, d'une fissure non plane fluctuant autour d'une surface moyenne $h = h(x_1)$ qui s'écarte du plan Ox_1x_3 dans un milieu élastique isotrope infiniment étendu. La fissure est une rangée continue de trois types de dislocation non droites avec des vecteurs de Burgers infinitésimaux : les types 1 et 2 sont des coins en moyenne de nature différente (1 obéissant au mode I et 2 au mode II) et le type 3 est constitué de vis en moyenne obéissant au mode III. Les dislocations sont orientées dans la direction x_3, ont une forme arbitraire petite $\xi = \xi(x_1, x_3)$ étalée (à la cote moyenne $h(x_1)$) dans des plans x_2x_3. Les champs de déplacement et de contrainte de trois dislocations, avec une forme arbitraire et un caractère moyen coin ou vis, sont d'abord donnés. Des expressions pour la contrainte au niveau du front de fissure et la force d'extension G de la fissure par unité de longueur du front de fissure sont également données. Une formule d'une moyenne spatiale de G, $< G >$, est établie dans le cas particulier d'une fissure non plane dont le front est segmenté. Des configurations de fissure non planes, pour lesquelles $< G >$ a une valeur plus élevée que celle correspondant à une fissure plane dans le plan Ox_1x_3, sont mises en évidence par la présente étude corroborant ainsi l'occurrence des fissures non planes abondamment observées dans des matériaux réels.

Mots-clés : *Propagation et arrêt de la fissure, Force d'extension de la fissure, Dislocations, mécanique de la rupture, Méthodes d'énergies*

I - INTRODUCTION

A planar crack in a solid under general loading can be analysed using a combination of three simple loading modes: tension perpendicular to the crack (mode I), shear parallel to crack applied perpendicularly to crack front (mode II) and shear parallel to crack directed along crack front (mode III). Explicit expressions for the stress at crack tip and crack extension force G per unit length of the crack front are available [1 to 3]. It is found experimentally that a certain amount of mode I is required for crack motion initiation. Although planar fracture under mode I loading is quite well understood, fracture in real materials generally occurs on a non-planar surface. Almost all experimentalists face non-planar surface when investigating broken

specimens. On the scientific side, the conditions (crack geometries, loading modes …) under which such cracks develop are not well understood. Of particular interest are methods leading to expressions for the stress about the crack front and crack extension force. The values taken by these quantities, when compared with those corresponding to the planar crack, could then explain the occurrence of non-planar cracks in real materials.

Consider a fracture specimen with large dimensions to which a Cartesian system x_i with origin O is attached; apply externally to specimen a tension σ_{22}^a in the x_2- direction and a shear σ_{23}^a along x_3: under such conditions fracture over large distance occurs on a non-planar surface $x_2 = \xi(x_1, x_2)$ that fluctuates about an average plane Ox_1x_3. Fracture is said to develop under mixed mode I+III loading. The fluctuation ξ is generally small ($1\mu m$ approximately) but spatial derivatives of ξ ($\partial\xi/\partial x_3$ for instance, assuming the crack to propagate along the x_1- direction) can be very large leading to a strong roughness of the broken surface even under very small shear by tension ratio $M_{13} \equiv \sigma_{23}^a / \sigma_{22}^a$ ($\approx 6\%$). These observations are derived from numerous experiments performed under various different conditions ([4 to 7], among others). Laboratory fracture experiments on large specimens under mixed mode I+II+III loading are uncommon. However, based on observations of numerous broken surfaces including mixed modes I+II ([8 to 11], for a revue see [5]) and I+III (as referenced above), one can anticipate the non-planar fracture surface in a specimen broken under mixed mode I+II+III loading to have the same features as those observed under mixed mode I+III with the main exception that the average fracture plane is inclined with respect to Ox_1x_3. Hence, when applying to specimen a shear σ_{12}^a in the x_1- direction, the average fracture surface will depart from x_1x_3.

The study of fracture in mixed mode I+III or I+II+III loading in solids requires a non-planar crack model that provides expressions for physical quantities pertinent to discuss crack propagation. For this purpose, a relevant quantity is the crack extension force per unit length of the crack front (or energy release rate) G. Since fracture proceeds through the motion of a macroscopic length of the crack front, it appears necessary to calculate an average $<G>$ and look for non-planar crack configurations that maximize $<G>$. These configurations may then be confronted with experiments.

A number of theoretical analyses devoted to non-planar cracks have been published. Works by Gao [12], Xu et al. [13], Ball and Larralde [14] and

Movchan et al. [15] consider a non-planar crack that fluctuates smoothly about imposed average fracture plane Ox_1x_3 (in our notation) under general loading (mixed mode I+II+III loading) except Ball and Larralde [14] which restrict themselves to mode I only. ξ and its spatial derivatives $\partial\xi/\partial x_1$ and $\partial\xi/\partial x_3$ are assumed small and linear expressions for the stress intensity factor (SIF) are given. These results have a narrow application. Actually these apply to a crack that propagates essentially under mode I loading but whose front, for various possible reasons, suffers a slight perturbation. Indeed, when a mode II loading (in addition to mode I) is applied to a planar crack located in x_1x_3, the subsequent fracture propagation path departs from x_1x_3 [16, 17] and condition ξ small is violated; for applied mode III as mentioned earlier, ξ is generally small but $\partial\xi/\partial x_3$ measured in the crack front x_3 − direction may be large even under M_{13} small.

In addition to these previous analyses, there exists theoretical works on non-planar fracture that impose ξ small only, with no restriction on its spatial derivatives (Lazarus et al. [18], Anongba [19]). Lazarus et al. [18] consider an initially planar semi-infinite straight edge crack (crack front in the x_3-direction) that adopts a non-planar configuration after fracture propagation over a short distance δ (in their notation), the new crack surface $\xi = \xi(\delta, x_3)$ (in our notation) being δ and x_3 dependent. The only small parameter is δ (or equivalently ξ); there is no restriction on the spatial derivatives of ξ. They provide stress intensity factors to first order in δ and use the usual plane strain relation to estimate the crack extension force G. Their approximate formula for G is written to second order in a parameter, denoted $d\gamma/d\delta$ by them, that is a measure of the derivative of the crack-front twist angle with respect to crack extension. The obtained relation overestimates actual rotation rates by nearly 3 orders of magnitude [18]. However they obtained a quiet good value of the global rotation rate by a more complex criterion based on the maximization of $<G>$ and SIF expressions for three or four point bending experiments.

We have previously considered a model of non-planar crack of finite length under mode I loading that fluctuates about an average plane [20 to 22]; the crack has a sinusoidal front perpendicular to the direction of fracture propagation and consists of a continuous distribution of sinusoidal edge dislocations [23]. The stress field of a sinusoidal edge dislocation leads to the stress about the crack front and crack extension force. The same approach is maintained in a recent work [19] extending to mixed mode I+III loading; the

crack front, instead of being simply sinusoidal, can now be arbitrary. The crack consists of a continuous distribution of infinitely long type 1 and 2 dislocations with edge and screw average characters. The dislocations are perpendicular to the x_1- direction of fracture propagation, have an arbitrary periodic small shape $\xi = \xi(x_3)$ (independent of x_1) spreading in the x_2x_3- plane and their portions may be arbitrarily inclined with respect to the x_3- direction. There is no restriction on the spatial derivatives of ξ ($\partial\xi/\partial x_3$ and $\partial^2\xi/\partial x_3^2$ particularly: see Section 5.1 in [19]). Dislocations 1 have an edge average character and respond to mode I loading; dislocations 2 have a screw average character and respond to mode III. The displacement and stress fields of two dislocations, with arbitrary shape and average character of edge or screw type, are given. Expressions for the stress about the crack front and crack extension force G per unit length of the crack front are also given. Formula for $<G>$, a spatial average of G, is provided for one special crack having a segmented front. Conditions under which $<G>$ is maximum conform to experimental measurements of crack-front twist angle versus applied stress.

Our method of analysis [19, 20] can be extended in a straightforward manner to mixed mode I+II+III loading; this is the goal of the present work that aims at providing explicit expressions for elastic fields of the crack dislocations, crack-tip stress and crack extension force G. This introduces a new type of sinusoidal edge II dislocation, responding to mode II loading, perpendicular to the x_1- direction and spreading in the x_2x_3- plane. Our modelling consider a crack whose surface f is given by $f(x_1,x_3) = \xi(x_1,x_3) + h(x_1)$ where ξ is a function of x_1 and x_3 oscillating about the value zero and taking small positive and negative values. h depends on x_1 only, odd (for definiteness) and taking arbitrary values. The average fracture surface is therefore defined by the equation $x_2 = h(x_1)$. The crack consists of a continuous distribution of three types of dislocation with infinitesimal Burgers vectors: types 1 and 2 are edges on average and different in nature (1 for the mode I loading and 2 for mode II) and type 3 corresponds to screws on average associated with mode III loading. The dislocations are long perpendicular to the x_1- direction; the one located at $x_1 = x_1^{'}$ spreads in the x_2x_3- plane in the form $\xi = \xi(x_1^{'}, x_3)$ with an average elevation (with respect to Ox_1x_3) given by $x_2 = h(x_1^{'})$. Elastic fields of the three types of dislocation are given in

Sections 2, 3 and 4; we first express the plastic distortion and obtain the associated displacement field using a method developed by Mura [24] as explained in Section 2.2. In Section 5 our crack model and analysis are presented; explicit expressions for the stress about the crack front and crack extension force G are provided. Section 6 deals with special cracks captured by the modelling with a more detailed description for G and associated spatial average value $< G >$. Concluding remarks are given in Section 7.

II – DISPLACEMENT AND STRESS FIELDS DUE TO A DISLOCATION OF EDGE I AVERAGE CHARACTER

II-1. Plastic distortion

We consider a dislocation with Burgers vector $(0,b,0)$ lying indefinitely in the x_3- direction and spreading in the x_2x_3- plane at the origin in the form of a Fourier series

$$f = \sum_n \left(\xi_n \sin \kappa_n x_3 + \delta_n \cos \kappa_n x_3\right) + h \equiv \xi + h \quad . \tag{2.1}$$

Here h and n are real and positive integer respectively; κ_n a wave number and ξ_n and δ_n are amplitudes. We assume ξ to be small and express the plastic distortion $\beta_{ij}^*(\vec{x})$ to first order in ξ; this gives

$$\beta_{12}^*(\vec{x}) = b\delta(x_1)H(x_2-h) - b\xi\delta(x_1)\delta(x_2-h) \tag{2.2}$$

and the other components of $\beta_{ij}^*(\vec{x})$ are zero, where δ and H are the Dirac delta function and the Heaviside step function, respectively. Here, the first term is due to a straight edge dislocation displaced by $x_2 = h$ from the origin. The corresponding displacement can be derived by replacing x_2 by $x_2 - h$ in the displacement of an edge dislocation at the origin (in the present geometry, see [23]). We shall therefore concentrate on the second term denoted $\beta_{12}^{*\xi}$. Its Fourier form may be written as

$$\beta_{12}^{*\xi}(\vec{x}) = \sum_{n} \sum_{k_{3n}=-\infty}^{\infty} \int_{-\infty}^{\infty}\int_{-\infty}^{\infty} \left(\overline{\beta}_{12}^{*\xi_n}(k_1,k_2,k_{3n}) + \overline{\beta}_{12}^{*\delta_n}(k_1,k_2,k_{3n})\right)$$

$$\times e^{i(k_1x_1+k_2x_2+k_{3n}\kappa_n x_3)} dk_1 dk_2 \qquad (2.3)$$

where

$$\overline{\beta}_{12}^{*\xi_n}(k_1,k_2,k_{3n}) = \frac{\kappa_n}{2\pi} \int_{-\pi/\kappa_n}^{\pi/\kappa_n} e^{-ik_{3n}\kappa_n x_3} dx_3 \frac{1}{(2\pi)^2} \int_{-\infty}^{\infty}\int_{-\infty}^{\infty} e^{-i(k_1x_1+k_2x_2)}$$

$$\times\left(-b\xi_n \sin\kappa_n x_3 \delta(x_1)\delta(x_2-h)\right) dx_1 dx_2 \qquad (2.4)$$

and

$$\overline{\beta}_{12}^{*\delta_n}(k_1,k_2,k_{3n}) = \frac{\kappa_n}{2\pi} \int_{-\pi/\kappa_n}^{\pi/\kappa_n} e^{-ik_{3n}\kappa_n x_3} dx_3 \frac{1}{(2\pi)^2} \int_{-\infty}^{\infty}\int_{-\infty}^{\infty} e^{-i(k_1x_1+k_2x_2)}$$

$$\times\left(-b\delta_n \cos\kappa_n x_3 \delta(x_1)\delta(x_2-h)\right) dx_1 dx_2; \qquad (2.5)$$

k_1 and k_2 are real and k_{3n} is a natural number. $\overline{\beta}_{12}^{*\xi_n}$ and $\overline{\beta}_{12}^{*\delta_n}$ are non zero only when $k_{3n} = \pm 1$ and equal to $\pm \exp(-ik_2h) ib\xi_n / 2(2\pi)^2$ and $-\exp(-ik_2h) b\delta_n / 2(2\pi)^2$ respectively. The Fourier form of $\beta_{12}^{*\xi}(\vec{x})$ may be arranged to read

$$\beta_{12}^{*\xi}(\vec{x}) = -\frac{b}{2(2\pi)^2} \sum_{n} \int_{-\infty}^{\infty}\int_{-\infty}^{\infty} \left(z_n e^{i(k_1x_1+k_2(x_2-h)-\kappa_n x_3)} + \bar{z}_n e^{i(k_1x_1+k_2(x_2-h)+\kappa_n x_3)}\right) dk_1 dk_2 \qquad (2.6)$$

where $z_n = \delta_n + i\xi_n$ and $\bar{z}_n = \delta_n - i\xi_n$.

II-2. Displacement and stress fields

The displacement $u_m(\vec{x})$ (m = 1, 2, 3) due to a plastic distortion of the form $\beta_{ij}^{*}(\vec{x}) = \overline{\beta}_{ij}^{*}(\vec{k})\ e^{i\vec{k}\vec{x}}$ where $\vec{k} = (k_1, k_2, k_3)$ has been obtained by Mura [24] to be

$$u_m(\vec{x}) = -ik_l c_{klji} L_{mk}(\vec{k}) \overline{\beta}_{ij}^{*}(\vec{k})\ e^{i\vec{k}\vec{x}}. \qquad (2.7)$$

For isotropic material,

$$L_{mk}(\vec{k}) = \frac{\delta_{km}(\lambda+2\mu)k^2 - k_k k_m(\lambda+\mu)}{\mu(\lambda+2\mu)k^4} \tag{2.8}$$

where $k^2 = k_1^2 + k_2^2 + k_3^2$ and

$$c_{klji} = \lambda\delta_{kl}\delta_{ji} + \mu\delta_{kj}\delta_{li} + \mu\delta_{ki}\delta_{lj}, \tag{2.9}$$

δ_{ij} being the Kronecker delta and λ and μ are Lamé constants. According to (2.7), $u_m(\vec{x}) = -ik_l c_{kl21} L_{mk}(\vec{k})\bar{\beta}_{12}^*(\vec{k})\ e^{i\vec{k}\vec{x}}$ if β_{12}^* is given as $\bar{\beta}_{12}^*(\vec{k})\ e^{i\vec{k}\vec{x}}$. In the present case however β_{12}^* is given by (2.6). The linear theory of elasticity allows for the superposition of solutions, so that the corresponding solution may be written as

$$u_m^{\xi}(\vec{x}) = -\frac{b}{2(2\pi)^2}\sum_n \int_{-\infty}^{\infty}\int_{-\infty}^{\infty} \Big(-ik_l' c_{kl21} L_{mk}(\vec{k}')z_n e^{i\vec{k}'\vec{x}_h} - ik_l\, c_{kl21} L_{mk}(\vec{k})\bar{z}_n e^{i\vec{k}\vec{x}_h}\Big)dk_1 dk_2, \tag{2.10}$$

in which $\vec{k}' = (k_1' = k_1, k_2' = k_2, k_3' = -\kappa_n)$, $\vec{k} = (k_1, k_2, k_3 = \kappa_n)$ and $\vec{x}_h = (x_1, x_2 - h, x_3)$. With (2.8) and (2.9), we may arrange (2.10) to read

$$u_i^{\xi}(\vec{x}) = \frac{b}{4\pi(1-\nu)}\sum_n \left(\xi_n \sin\kappa_n x_3 + \delta_n \cos\kappa_n x_3\right)\left\|(1-2\nu) - (x_1\delta_{i1} + (x_2-h)\delta_{i2})\frac{\partial}{\partial x_i}\right\| \times \frac{\partial}{\partial(x_1\delta_{i2} + x_2\delta_{i1})} I_n \tag{2.11}$$

and

$$u_3^{\xi}(\vec{x}) = -\frac{b}{4\pi(1-\nu)}\sum_n \frac{\partial}{\partial x_3}\left(\xi_n \sin\kappa_n x_3 + \delta_n \cos\kappa_n x_3\right)\ (x_2-h)\frac{\partial}{\partial x_1} I_n, \tag{2.12}$$

where

$$I_n = \frac{1}{2\pi}\int_{-\infty}^{\infty}\int_{-\infty}^{\infty} \frac{1}{k_1^2 + k_2^2 + \kappa_n^2} e^{i(k_1 x_1 + k_2(x_2-h))}dk_1 dk_2 = K_0[\kappa_n r], \tag{2.13}$$

the subscript i taking the values 1 or 2 in (2.11); the term in $\| \|$ is an operator that acts on the factor with I_n; $r^2 = x_1^2 + (x_2 - h)^2$. $K_n[x]$ is the *n*th-order modified Bessel function usually so denoted and δ_{ij} is the Kronecker delta. Finally, the total displacement at $\vec{x} = (x_1, x_2, x_3)$ takes the form:

$$u_i(\vec{x}) = u_i^{0h}(\delta_{i1} + \delta_{i2}) + \frac{b}{4\pi(1-\nu)}\left(\frac{x_1\delta_{i2} + (x_2 - h)\delta_{i1} + x_1(x_2 - h)\delta_{i3}}{r}\right)$$
$$\times \sum_n \left\| \delta_{i1} + \delta_{i2} + \delta_{i3}\frac{\partial}{\partial x_3} \right\| A_n\kappa_n\left(-\frac{\kappa_n(x_1^2\delta_{i1} + (x_2 - h)^2\delta_{i2})}{r}K_0[\kappa_n r]\right.$$
$$\left. + \left((2\nu - 1)(\delta_{i1} + \delta_{i2}) - \frac{2(x_1^2\delta_{i1} + (x_2 - h)^2\delta_{i2})}{r^2} + \delta_{i3}\right)K_1[\kappa_n r]\right), \quad (2.14)$$

subscript i = 1, 2 and 3; $A_n = \xi_n \sin\kappa_n x_3 + \delta_n \cos\kappa_n x_3$; the term in $\| \|$ is an operator that acts on A_n; ν is Poisson's ratio. u_i^{0h} is the displacement due to a straight edge dislocation displaced by $x_2 = h$ from the origin:

$$u_1^{0h}(\vec{x}) = -\frac{b(2\nu - 1)}{8\pi(1-\nu)}\ln\left(r^2\right) - \frac{b}{4\pi(1-\nu)}\frac{x_1^2}{r^2},$$
$$u_2^{0h}(\vec{x}) = -\frac{b}{2\pi}\tan^{-1}\left(\frac{x_1}{x_2 - h}\right) - \frac{b}{4\pi(1-\nu)}\frac{x_1(x_2 - h)}{r^2}. \quad (2.15)$$

The stress field can be obtained by differentiating the displacement. We find:

$$\sigma_{ii}(\vec{x}) = \sigma_{ii}^{0h}(\vec{x}) + \frac{Cx_1(x_2 - h)}{r^2}\sum_n \kappa_n A_n\left(\kappa_n\left[-(\delta_{i1} + \delta_{i2}) + 2\nu\delta_{i3}\right.\right.$$
$$\left. + \frac{4(x_1^2\delta_{i1} + (x_2 - h)^2\delta_{i2})}{r^2}\right]K_0[\kappa_n r] + \frac{1}{r}\left[-2(\delta_{i1} + \delta_{i2}) + 4\nu\delta_{i3}\right.$$
$$\left.\left. + \kappa_n^2\left(x_1^2(\delta_{i1} - \delta_{i3}) + (x_2 - h)^2(\delta_{i2} - \delta_{i3})\right) + \frac{8(x_1^2\delta_{i1} + (x_2 - h)^2\delta_{i2})}{r^2}\right]K_1[\kappa_n r]\right),$$
$$\sigma_{12}(\vec{x}) = \sigma_{12}^{0h}(\vec{x}) + C\sum_n \kappa_n A_n\left(\kappa_n\left[-\nu + \frac{4x_1^2(x_2 - h)^2}{r^4}\right]K_0[\kappa_n r]\right.$$

$$+\frac{1}{r}\left[-1+\frac{\kappa_n^2 x_1^2 (x_2-h)^2}{r^2}+\frac{8x_1^2(x_2-h)^2}{r^4}\right]K_1[\kappa_n r]\Bigg),$$

$$\sigma_{j3}(\vec{x}) = C\frac{x_1\delta_{j2}+(x_2-h)\delta_{j1}}{r}\sum_n \kappa_n \frac{\partial A_n}{\partial x_3}\Bigg(-\frac{\kappa_n(x_1^2\delta_{j1}+(x_2-h)^2\delta_{j2})}{r}K_0[\kappa_n r]$$

$$+\left[\nu(\delta_{j1}+\delta_{j2})-\frac{2(x_1^2\delta_{j1}+(x_2-h)^2\delta_{j2})}{r^2}\right]K_1[\kappa_n r]\Bigg), \quad (2.16)$$

where subscripts i and j take the values (1, 2 and 3) and (1 and 2) respectively, $C=\mu b/2\pi(1-\nu)$ and σ_{ij}^{0h} is the stress due to the straight edge dislocation displaced by $x_2=h$ from the origin:

$$\sigma_{12}^{0h}(\vec{x}) = C\frac{(x_2-h)(x_1^2-(x_2-h)^2)}{r^4},$$

$$\sigma_{ii}^{0h}(\vec{x}) = C\frac{x_1}{r^2}\left(\frac{x_1^2(\delta_{i1}+\delta_{i2})+(x_2-h)^2(-\delta_{i1}+3\delta_{i2})}{r^2}+2\nu\delta_{i3}\right),\ i=1,\ 2 \text{ and } 3. \quad (2.17)$$

Note that $\sigma_{j3}^{0h}(\vec{x})=0$ (j = 1 and 2).

We indicate here a useful observation. From equations (2.14) and (2.16), those due to a dislocation with the form $f=\xi_n\sin\kappa_n x_3+\delta_n\cos\kappa_n x_3+h$ may be obtained by removing the symbol Σ (in (2.14) and (2.16)). Conversely from the knowledge of the elastic fields due to a dislocation with the simple form $f=\xi_n\sin\kappa_n x_3+h$, we arrive at those corresponding to a dislocation with the more general form (2.1), simply by adding Σ to the fields and writing $\xi_n\sin\kappa_n x_3+\delta_n\cos\kappa_n x_3$ instead of $\xi_n\sin\kappa_n x_3$ and $\kappa_n(\xi_n\cos\kappa_n x_3-\delta_n\sin\kappa_n x_3)$ instead of $\kappa_n\xi_n\cos\kappa_n x_3$.

III – DISPLACEMENT AND STRESS FIELDS DUE TO A DISLOCATION OF EDGE II AVERAGE CHARACTER

III-1. Plastic distortion

We consider a dislocation with Burgers vector $(b,0,0)$ lying in the x_3- direction and spreading in the x_2x_3- plane at the origin in the Fourier

series form (2.1). As indicated at the end of Section 2.2, the elastic fields of this dislocation can be derived from those due to a sinusoidal dislocation located at the origin with the same Burgers vector, lying in the x_2x_3- plane and defined by $x_2 = \xi_n \sin \kappa_n x_3$ ($h = 0$), ***Figure 1***. We first treat this simple case. Let the sinusoidal dislocation be introduced in the medium by sliding the part of the material $x_1 < 0$ and $x_2 > \xi_n \sin \kappa_n x_3$ by $\vec{b} = (b,0,0)$ and the unit normal to the surface $x_2 = \xi_n \sin \kappa_n x_3$ (denoted S and hachured on ***Figure 1***), at an arbitrary point $P = (x_1, \xi_n \sin \kappa_n x_3, x_3)$,be equal to $\vec{n} = 1/\sqrt{1+(\xi_n \kappa_n \cos \kappa_n x_3)^2}$ $(0, -1, \xi_n \kappa_n \cos \kappa_n x_3)$ pointing to the negative x_2-direction. The plastic distortion β_{ij}^* is written by Mura [25] as

$$\beta_{ij}^*(\vec{x}) = -b_j n_i \delta(\rho(\vec{x})) \tag{3.1}$$

where b_j and n_i are the component of the Burgers vector $\vec{b}$ of the dislocation and $\vec{n}$ respectively; $\rho(\vec{x})$ is the distance from the position defined by $\vec{x}$ to the surface S measured along a direction perpendicular to S (i.e., parallel to $\vec{n}$) and δ is the one–dimensional Dirac delta function, being unbounded when $\vec{x}$ is on S (i.e., $\rho(\vec{x}) = 0$) and zero otherwise. There are two non-zero components of the plastic distortion (by using (3.1) and adding the Heaviside step function):

$$\beta_{21}^*(\vec{x}) = \frac{b}{1+(\xi_n \kappa_n \cos \kappa_n x_3)^2} \delta(x_2 - \xi_n \sin \kappa_n x_3) \; H(-x_1) \tag{3.2}$$

and

$$\beta_{31}^*(\vec{x}) = -\xi_n \kappa_n \cos \kappa_n x_3 \; \beta_{21}^*(\vec{x}) \tag{3.3}$$

where H is the Heaviside step function; we assume the shape $\xi = \xi_n \sin \kappa_n x_3$ to be small: this assumption is common to the three types of dislocation considered in this study. In addition, particular to the dislocation of edge II average character, we also consider $\partial \xi / \partial x_3$ small. This reduces coefficient $[1/1+(\xi_n \kappa_n \cos \kappa_n x_3)^2]$ to unity in (3.2); corresponding Fourier forms used in the sequel are

$$\beta_{21}^{*}(\vec{x}) = \frac{b}{(2\pi)^2} \int_{-\infty}^{\infty} \int_{-\infty}^{\infty} \frac{1}{ik_1} \left[-1 - \frac{\xi_n k_2}{2} (e^{-i\kappa_n x_3} - e^{i\kappa_n x_3}) \right] e^{i(k_1 x_1 + k_2 x_2)} dk_1 dk_2 \tag{3.4}$$

and

$$\beta_{31}^{*}(\vec{x}) = \frac{b\kappa_n \xi_n}{8\pi^2} \int_{-\infty}^{\infty} \int_{-\infty}^{\infty} \frac{1}{ik_1} \left[e^{-i\kappa_n x_3} + e^{i\kappa_n x_3} \right] e^{i(k_1 x_1 + k_2 x_2)} dk_1 dk_2 \tag{3.5}$$

respectively, where k_1 and k_2 are real.

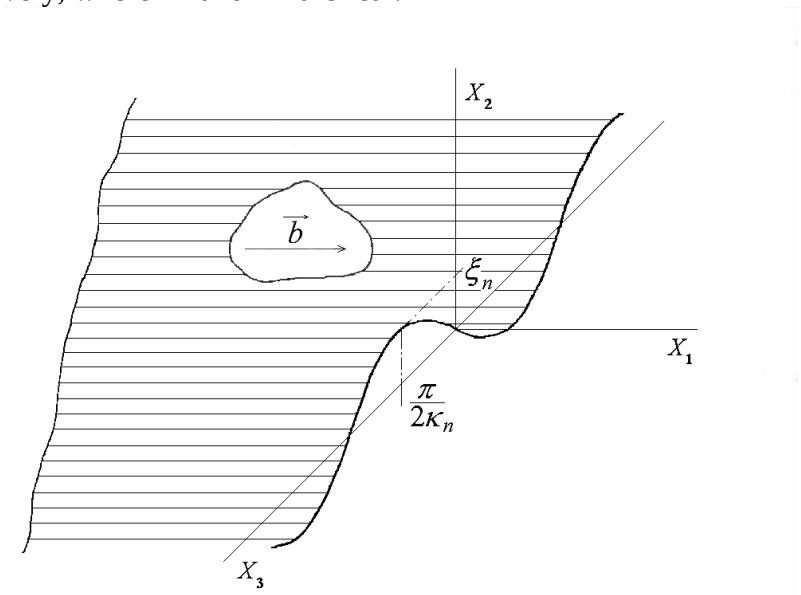

Figure 1 : *A sinusoidal edge II dislocation lying in the* $x_2 x_3$ *– plane at the origin with a Burgers vector in the* x_1 *– direction*

III-2. Displacement and stress fields

With two non zero components β_{21}^{*} and β_{31}^{*}, the displacement (2.7) reads

$$\bar{u}_m(\vec{x}) = -i\ \mu\ (k_1 L_{m2} + k_2 L_{m1})\ \bar{\beta}_{21}^{*}\ e^{i\vec{k}\vec{x}} - i\ \mu\ (k_1 L_{m3} + k_3 L_{m1})\ \bar{\beta}_{31}^{*}\ e^{i\vec{k}\vec{x}} . \tag{3.6}$$

In the present study β_{21}^{*} and β_{31}^{*}, as given by their Fourier forms (3.4) and (3.5), are integrals of expressions of the form $\bar{\beta}_{ij}^{*}(\vec{k})\ e^{i\vec{k}\vec{x}}$. The linear theory of elasticity allows for the superposition of solutions, so that the displacements

$u_m(\vec{x})$ to the present problem are similar integrals of displacements of the form $\bar{u}_m$. We thus obtain at once

$$u_m = \frac{\mu b}{(2\pi)^2}\int_{-\infty}^{\infty}\int_{-\infty}^{\infty}\left\{(\delta_{m1}+\delta_{m2})\left[L_{m2}(\vec{k}_0)+\frac{k_2}{k_1}L_{m1}(\vec{k}_0)\right]-\frac{\xi_n}{2}\left(e^{i\kappa_n x_3}+(-1)^{1+\delta_{m3}}e^{-i\kappa_n x_3}\right)\right.$$
$$\left.\times\left[k_2 L_{m2}(\vec{k})+\frac{k_2^2}{k_1}L_{m1}(\vec{k})+\kappa_n L_{m3}(\vec{k})+\frac{\kappa_n^2}{k_1}L_{m1}(\vec{k})\right]\right\}e^{i(k_1x_1+k_2x_2)}dk_1dk_2 \tag{3.7}$$

where the subscript m takes the values 1, 2 or 3, $\vec{k}_0=(k_1,k_2)$ and $\vec{k}=(k_1,k_2,k_3=\kappa_n)$. With (2.8), this becomes

$$u_m = \frac{b}{(2\pi)^2}\int_{-\infty}^{\infty}\int_{-\infty}^{\infty}\left\{(\delta_{m1}+\delta_{m2})\left[\frac{k_2}{k_m k_0^2}-\frac{1}{1-\nu}\frac{k_m k_2}{k_0^4}\right]-\frac{\xi_n}{2}\left(e^{i\kappa_n x_3}+(-1)^{1+\delta_{m3}}e^{-i\kappa_n x_3}\right)\right.$$
$$\left.\times\left[\frac{k_2^2(\delta_{m1}+\delta_{m2})+\kappa_n^2(\delta_{m1}+\delta_{m3})}{k_m(k_0^2+\kappa_n^2)}-\frac{1}{1-\nu}\frac{k_m(k_2^2+\kappa_n^2)}{(k_0^2+\kappa_n^2)^2}\right]\right\}e^{i(k_1x_1+k_2x_2)}dk_1dk_2 \tag{3.8}$$

where $k_0^2=k_1^2+k_2^2$. Further calculations involve the following identities:

$$-\frac{1}{2\pi i}\int_{-\infty}^{\infty}\int_{-\infty}^{\infty}\frac{1}{k_1(k_1^2+k_2^2+\kappa_n^2)}e^{i(k_1x_1+k_2x_2)}dk_1dk_2=\int_{x_1}^{\infty}K_0[\kappa_n\sqrt{x^2+x_2^2}]\;dx\equiv\bar{I}(x_1,x_2)$$
,

$$\frac{1}{2\pi}\int_{-\infty}^{\infty}\int_{-\infty}^{\infty}\frac{1}{k_1^2+k_2^2+\kappa_n^2}e^{i(k_1x_1+k_2x_2)}dk_1dk_2=K_0[\kappa_n r_0]$$
,

$$\frac{\kappa_n}{\pi}\int_{-\infty}^{\infty}\int_{-\infty}^{\infty}\frac{1}{(k_1^2+k_2^2+\kappa_n^2)^2}e^{i(k_1x_1+k_2x_2)}dk_1dk_2=\kappa_n\int_{x_1}^{\infty}xK_0[\kappa_n\sqrt{x^2+x_2^2}]\;dx=r_0K_1[\kappa_n r_0]$$
,

$$\frac{1}{\pi i}\int_{-\infty}^{\infty}\int_{-\infty}^{\infty}\frac{k_i}{(k_1^2+k_2^2+\kappa_n^2)^2}e^{i(k_1x_1+k_2x_2)}dk_1dk_2=x_iK_0[\kappa_n r_0]$$
, (3.9)

where $r_0^2=x_1^2+x_2^2$ and the subscript i takes the values 1 or 2. The terms of zero order with respect to ξ_n in the displacement (3.8) correspond to the

straight edge dislocation (see [25] for instance). The calculations in (3.8) lead to the displacement of the sinusoidal dislocation at the origin with Burgers vector $^{(b,0,0)}$. The displacement due to a dislocation of edge II average character with form (2.1) may then be expressed as:

$$u_1(\vec{x}) = u_1^{0h} + \frac{b}{4\pi(1-\nu)}\sum_n A_n\Bigg[2(1-\nu)\,\|\,-\kappa_n^2 + \frac{\partial^2}{\partial x_2^2}\,\|\,\bar{I}(x_1, x_2-h) - \frac{\kappa_n^2 x_1^3}{r^2}K_0[\kappa_n r] + \frac{\kappa_n x_1}{r}(-1+\frac{2(x_2-h)^2}{r^2})K_1[\kappa_n r]\Bigg],$$

$$u_2(\vec{x}) = u_2^{0h} + \frac{b}{4\pi(1-\nu)}\sum_n A_n\Bigg[-\frac{\kappa_n^2(x_2-h)x_1^2}{r^2}K_0[\kappa_n r] + \frac{\kappa_n(x_2-h)}{r}\left(-(1+2\nu)+\frac{2(x_2-h)^2}{r^2}\right)K_1[\kappa_n r]\Bigg],$$

$$u_3(\vec{x}) = \frac{b}{4\pi(1-\nu)}\sum_n \frac{\partial}{\partial x_3}A_n\Bigg[(-1+2\nu)K_0[\kappa_n r] + \frac{\kappa_n x_1^2}{r}K_1[\kappa_n r]\Bigg]. \qquad (3.10)$$

The term in $\|\ \|$ is an operator that acts on $\bar{I}$ defined in (3.9). $r^2 = x_1^2 + (x_2-h)^2$ and u_i^{0h} is the displacement due to a straight edge dislocation displaced by $x_2 = h$ from the origin:

$$u_1^{0h}(\vec{x}) = \frac{b}{2\pi}\tan^{-1}\left(\frac{x_2-h}{x_1}\right) + \frac{b}{4\pi(1-\nu)}\frac{x_1(x_2-h)}{r^2},$$

$$u_2^{0h}(\vec{x}) = \frac{b(2\nu-1)}{8\pi(1-\nu)}\ln\left(r^2\right) + \frac{b}{4\pi(1-\nu)}\frac{(x_2-h)^2}{r^2}, \quad u_3^{0h} = 0. \qquad (3.11)$$

The stress field associated with (2.1) can be obtained by differentiating the displacement. We find:

$$\sigma_{12} = \sigma_{12}^{0h} + C\sum_n A_n\Bigg[(1-\nu)\,\|\,-\kappa_n^2\frac{\partial}{\partial x_2} + \frac{\partial^3}{\partial x_2^3}\,\|\,\bar{I} + \frac{\kappa_n^2 x_1(x_2-h)}{r^2}\left(2+\nu-\frac{4(x_2-h)^2}{r^2}\right)K_0$$

$$+\frac{\kappa_n x_1(x_2-h)}{r^3}\left(2(2+\nu)+\kappa_n^2 x_1^2-\frac{8(x_2-h)^2}{r^2}\right)K_1[\kappa_n r]\Bigg],$$

$$\sigma_{13}(\vec{x})=C\sum_n \kappa_n \frac{\partial}{\partial x_3}A_n\Bigg[(1-\nu)\,\|-\kappa_n+\frac{1}{\kappa_n}\frac{\partial^2}{\partial x_2^2}\,\|\,\bar{I}(x_1,x_2-h)-\frac{\kappa_n x_1^3}{r^2}K_0[\kappa_n r]$$
$$+\frac{x_1}{r}\left(-\nu+\frac{2(x_2-h)^2}{r^2}\right)K_1[\kappa_n r]\Bigg],$$

$$\sigma_{23}(\vec{x})=-C\frac{(x_2-h)}{r}\sum_n \kappa_n \frac{\partial}{\partial x_3}A_n\left[\frac{\kappa_n x_1^2}{r}K_0[\kappa_n r]+\left(2\nu+\frac{x_1^2-(x_2-h)^2}{r^2}\right)K_1[\kappa_n r]\right],$$

$$\sigma_{11}(\vec{x})=\sigma_{11}^{0h}(\vec{x})+C\sum_n A_n\Bigg[2\kappa_n^2\frac{x_1^2\left(x_1^2-(x_2-h)^2\right)}{r^4}K_0[\kappa_n r]$$
$$+\frac{\kappa_n}{r}\left(3+\frac{\kappa_n^2 x_1^4}{r^2}-\frac{4(x_2-h)^2\left(3x_1^2+(x_2-h)^2\right)}{r^4}\right)K_1[\kappa_n r]\Bigg],$$

$$\sigma_{22}(\vec{x})=\sigma_{22}^{0h}(\vec{x})+C\sum_n A_n\Bigg[\kappa_n^2\left(-(1-2\nu)+\frac{4x_1^2(x_2-h)^2}{r^4}\right)K_0[\kappa_n r]$$
$$+\frac{\kappa_n}{r}\left(-1+\frac{\kappa_n^2 x_1^2(x_2-h)^2}{r^2}+\frac{8x_1^2(x_2-h)^2}{r^4}\right)K_1[\kappa_n r]\Bigg],$$

$$\sigma_{33}(\vec{x})=\sigma_{33}^{0h}(\vec{x})+C\sum_n A_n\Bigg[\kappa_n^2\left(1-\frac{2\nu(x_2-h)^2}{r^2}\right)K_0[\kappa_n r]$$
$$+\frac{\kappa_n}{r}\left(-\kappa_n^2 x_1^2+\frac{2\nu\left(x_1^2-(x_2-h)^2\right)}{r^2}\right)K_1[\kappa_n r]\Bigg]. \qquad (3.12)$$

σ_{ij}^{0h} is the stress due to the straight edge dislocation displaced by $x_2=h$ from the origin:

$$\sigma_{12}^{0h}(\vec{x})=C\frac{x_1\left(x_1^2-(x_2-h)^2\right)}{r^4},\qquad \sigma_{11}^{0h}(\vec{x})=-C\frac{(x_2-h)\left(3x_1^2+(x_2-h)^2\right)}{r^4},$$

$$\sigma_{22}^{0h}(\vec{x})=C\frac{(x_2-h)\left(x_1^2-(x_2-h)^2\right)}{r^4},\qquad \sigma_{33}^{0h}(\vec{x})=-2C\nu\frac{(x_2-h)}{r^2}. \qquad (3.13)$$

Note that $\sigma_{13}^{0h} = \sigma_{23}^{0h} = 0$.

IV - DISPLACEMENT AND STRESS FIELDS DUE TO A DISLOCATION OF SCREW AVERAGE CHARACTER

We consider a dislocation with Burgers vector $(0,0,b)$ lying in the x_3- direction and spreading in the x_2x_3- plane at the origin in the Fourier series form (2.1). The only non-zero component of the plastic distortion is written to first order in ξ:

$$\beta_{13}^{*}(\vec{x}) = b\delta(x_1)H(x_2-h) - b\xi\delta(x_1)\delta(x_2-h) \tag{4.1}$$

that is identical to (2.2). Here, the first term is due to the straight screw dislocation displaced by $x_2 = h$ from the origin. The corresponding displacement can be derived by replacing x_2 by $x_2 - h$ in the displacement of a screw dislocation at the origin (see for instance [24]). The Fourier form of the second term is identical to that (2.6) of $\beta_{12}^{*\xi}$ (Section 2). To get the total displacement field, we proceed exactly as for the dislocation of edge I average character (Section 2). The result is

$$u_i(\vec{x}) = u_i^{0h}(\vec{x})\delta_{i3} + \frac{b}{4\pi(1-\nu)}\sum_n \left\| \kappa_n x_1\delta_{i3} + (\delta_{i1}+\delta_{i2})\frac{\partial}{\partial x_3} \right\| A_n$$
$$\times\left(\left((1-2\nu)\delta_{i1} + \kappa_n\delta_{i3}\right)K_0[\kappa_n r] + \frac{\kappa_n x_1(x_1\delta_{i1} + (x_2-h)\delta_{i2}) - 2(1-\nu)\delta_{i3}}{r}K_1[\kappa_n r] \right); \tag{4.2}$$

subscript $i = 1,\ 2$ and 3; u_3^{0h} is the displacement due to a straight screw dislocation displaced by $x_2 = h$ from the origin:

$$u_3^{0h}(\vec{x}) = \frac{b}{2\pi}\tan^{-1}\left(\frac{x_2-h}{x_1}\right). \tag{4.3}$$

The stress field can be obtained by differentiating the displacement. We get:

$$\sigma_{ii}(\vec{x}) = Cx_1\left(\frac{\delta_{i1}+\delta_{i2}}{r}+\delta_{i3}\right)\sum_n \kappa_n \frac{\partial A_n}{\partial x_3}\left(\kappa_n\left[-\frac{x_1^2\delta_{i1}+(x_2-h)^2\delta_{i2}}{r}+\delta_{i3}\right]K_0[\kappa_n r]\right.$$

$$\left.+\left[\frac{(-\delta_{i1}+\delta_{i2})(x_1^2-(x_2-h)^2)}{r^2}-2\nu\delta_{i2}-\frac{2}{r}\delta_{i3}\right]K_1[\kappa_n r]\right),$$

$$\sigma_{12}(\vec{x}) = C\frac{x_2-h}{r}\sum_n \kappa_n \frac{\partial A_n}{\partial x_3}\left(-\frac{\kappa_n x_1^2}{r}K_0[\kappa_n r]+\left[\nu-\frac{2x_1^2}{r^2}\right]K_1[\kappa_n r]\right),$$

$$\sigma_{j3}(\vec{x}) = \sigma_{j3}^{0h}(\vec{x}) + \sum_n \frac{CA_n\kappa_n}{r}\left(\frac{\kappa_n\left((x_1^2+\nu(x_2-h)^2)\delta_{j1}+(1-\nu)x_1(x_2-h)\delta_{j2}\right)}{r}K_0[\kappa_n r]\right.$$

$$\left.+\left[-\kappa_n^2\left(x_1^2\delta_{j1}+x_1(x_2-h)\delta_{j2}\right)+\frac{(1-\nu)\left(\left(x_1^2-(x_2-h)^2\right)\delta_{j1}+2x_1(x_2-h)\delta_{j2}\right)}{r^2}\right]K_1[\kappa_n r]\right). \quad (4.4)$$

Subscripts i and j take the values (1, 2 and 3) and (1 and 2) respectively and σ_{ij}^{0h} is the stress due to a straight screw dislocation displaced by $x_2 = h$ from the origin:

$$\sigma_{i3}^{0h}(\vec{x}) = \frac{\mu b}{2\pi}\left(\frac{x_1\delta_{i2}-(x_2-h)\delta_{i1}}{r^2}\right),\ i = 1 \text{ and } 2. \quad (4.5)$$

Note that $\sigma_{ii}^{0h}(\vec{x}) = 0$ (i = 1, 2 and 3) and $\sigma_{12}^{0h} = 0$.

V- ANALYSIS OF THE NON-PLANAR CRACK

V-1. The model

The dislocations with edge I and II (Sections 2 and 3) and screw (Section 4) average characters are now considered to be continuously distributed over the interval $x_1 = -a$ to a. The shape f of the dislocations depends on x_1 in the form

$$f = \xi(x_1, x_3) + h(x_1) = \sum_n \left(\xi_n(x_1)\sin\kappa_n(x_1)x_3 + \delta_n(x_1)\cos\kappa_n(x_1)x_3\right) + h(x_1). \quad (5.1)$$

It is understood in our crack analysis that ξ_n, δ_n, κ_n and h (introduced in (2.1)) are position dependent along x_1 in the dislocation distribution. The medium is assumed to be infinite, isotropic and elastic and subjected to uniform applied tension σ_{22}^a and shears σ_{12}^a and σ_{23}^a at infinity. The dislocation distribution function $D_i(x_1)$ ($i=1$ and 2 for the edges I and II and $i=3$ for the screws) gives the number of dislocations i in a small interval dx_1 about x_1 as $D_i(x_1)dx_1$. Dislocations 1, 2 and 3 have a Burgers vector $(0,b,0)$, $(b,0,0)$ and $(0,0,b)$ respectively and to anyone located at x_1 a running point $P=(x_1, f, x_3)$ (f being given by (5.1)) is associated. We are concerned with the problem of finding the equilibrium distributions D_i of the dislocations under the combined action of their mutual repulsions and the force exerted on them by σ_{22}^a, σ_{12}^a and σ_{23}^a. We may ask for zero total force at any point P on each of the infinitesimal dislocations or equally (as shown in [19]) ask for the crack faces to be traction free. The latter condition is found to be more convenient, it reads

$$\begin{cases} \bar{\sigma}_{12} - \partial f/\partial x_1 \bar{\sigma}_{11} - \partial f/\partial x_3 \bar{\sigma}_{13} = 0 \\ \bar{\sigma}_{22} - \partial f/\partial x_1 \bar{\sigma}_{12} - \partial f/\partial x_3 \bar{\sigma}_{23} = 0 \\ \bar{\sigma}_{23} - \partial f/\partial x_1 \bar{\sigma}_{13} - \partial f/\partial x_3 \bar{\sigma}_{33} = 0 \end{cases}. \qquad (5.2)$$

$\bar{\sigma}_{ij}$ stands for the total stress at any point (x_1, x_2, x_3) in the medium and is linked to D_i. In (5.2), we are only concerned with the points of the crack faces. We write $\bar{\sigma}_{ij}$ as

$$\bar{\sigma}_{ij} = \bar{\sigma}_{ij}^{(1)} + \bar{\sigma}_{ij}^{(2)} + \bar{\sigma}_{ij}^{(3)} \qquad (5.3$$

where

$$\bar{\sigma}_{ij}^{(n)}(x_1, x_2, x_3) = \sigma_{ij}^{(n)a} + \int_{-a}^{a} \sigma_{ij}^{(n)}(x_1 - x_1', x_2, x_3) D_n(x_1') dx_1' \qquad (n=1, 2 \text{ and } 3); \qquad (5.4)$$

here $\sigma_{ij}^{(n)}$ (n = 1,2 or 3) is the stress field produced by a dislocation displaced by ($x_2 - h$)from the origin with Burgers vector $(0,b,0)$, $(b,0,0)$ or $(0,0,b)$. $\sigma_{ij}^{(n)a}$, the applied stress, is equal to zero except $\sigma_{22}^{(1)a} = \sigma_{22}^a$, $\sigma_{12}^{(2)a} = \sigma_{12}^a$ and $\sigma_{23}^{(3)a} = \sigma_{23}^a$.

Figure 2 is a schematic representation of special cracks captured by the modelling. The cracks extend in the x_1- direction from $x_1=-a$ to a and must be considered to run indefinitely in the x_3- direction. The crack of ***Figure 2c*** is confined for illustration purpose in a parallelepiped of finite size. The crack shape in planes perpendicular to x_1 is described by ξ (***Figure 2c*** for example).

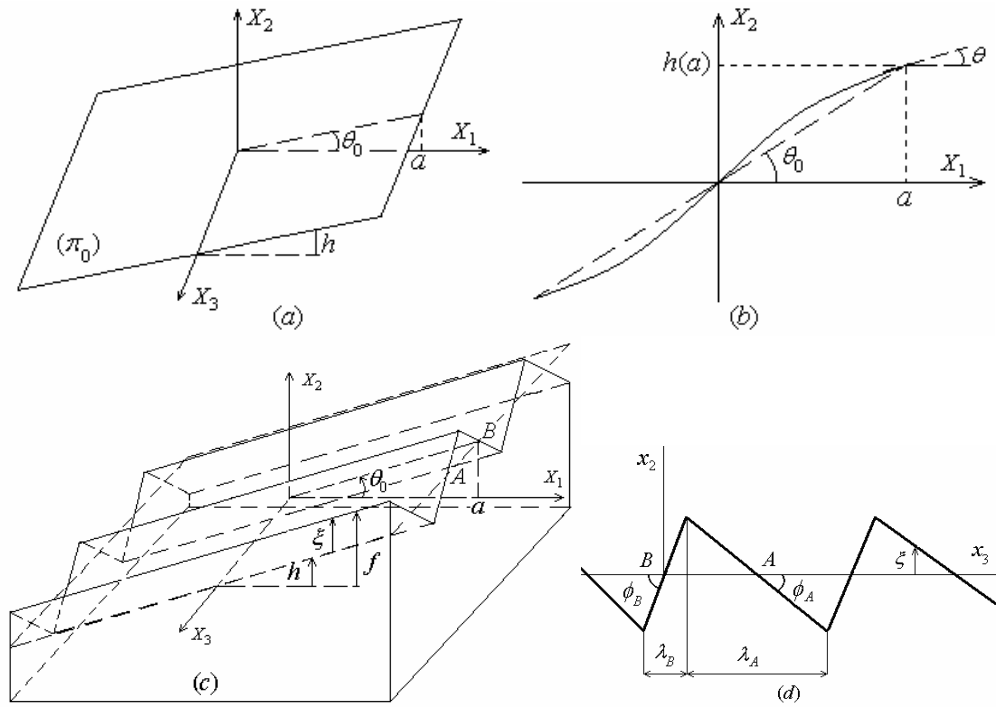

Figure 2 : *Simple special cracks. (a) Inclined planar crack π_0 (see text). (b) A non-planar crack (parallel to x_3) as h odd function of x_1 ($x_2=h(x_1)$). (c) Non-planar crack fluctuating about an average inclined plane π_0. The crack consists of planar facets; its fronts at $x_1=\pm a$ lie in x_2x_3- planes. At $x_1=a$, the crack front is characterized by inclination angles ϕ_A and ϕ_B (see (d)) at points A and B located on the average fracture plane. (d) Sketch of the crack front in (c) with B taken as origin. In this geometry (from (a) to (c)) the general loading of the crack systems corresponds to uniform applied σ_{22}^a, σ_{12}^a and σ_{23}^a at infinity in the x_2, x_1 and x_3 directions, respectively.*

Although ξ is given as a Fourier series in (5.1), it appears as a general function in expressions for both the stress about the crack front (Section 5.3) and the crack extension force G (Section 5.4). The shape f of the crack in planes perpendicular to x_3 is given by both ξ, through the x_1-dependence of positive quantities ξ_n, δ_n and κ_n (Equation (5.1)), and function $h = h(x_1)$. Since ξ is assumed to be small oscillating function, the average fracture plane is described correctly by the equation $x_2 = h(x_1)$. When $\xi = 0$, the crack dislocations are straight parallel to x_3 and distributed over the surface $x_2 = h(x_1)$ .Specific examples are (***Figure 2***):

- $h(x_1) = p_0 x_1$ ($p_0 \geq 0$) and $\xi = 0$. This corresponds to a planar crack π_0 (with a straight front parallel to x_3) rotated around Ox_3 by angle $\theta_0 = \tan^{-1} p_0$ from Ox_1x_3, ***Figure 2a***.
- $h(x_1)$ is an arbitrary function of x_1 and $\xi = 0$. The sketch in ***Figure 2b*** corresponds to h odd although this is not mandatory. Actually h odd conforms well to homogeneity of the medium, geometry of the applied loadings and D_i (5.7) approximations adopted in the present study.
- $h(x_1) = p_0 x_1$ ($p_0 \geq 0$) and $\xi = \xi(x_3)$ independent of x_1. The crack fluctuates about plane π_0 with a front spreading in planes parallel to x_2x_3 in the form ξ. In the example displayed in ***Figure 2c*** the crack consists of planar facets with inclination angles ϕ_A and ϕ_B (***Figure 2d***) at points *A* and *B* of the crack front located on the average fracture plane.

V-2. Dislocation distributions

Assume first that the dislocations are straight parallel to the x_3- direction $(\xi = 0)$ and $h(x_1) = p_0 x_1$ depends linearly on x_1 with p_0 positive constant (***Figure 2a***). We thus have a planar crack of finite extension, with straight fronts running indefinitely along x_3, rotated (from Ox_1x_3) about the positive x_3- direction by $\theta_0 = \tan^{-1} p_0$. The crack extends from $x_1 = -a$ to a and is subjected to mixed mode I+II+III with loadings applied at infinity. Under such conditions in (5.2) we have $\partial f / \partial x_1 = \partial h / \partial x_1 = p_0$, $\partial f / \partial x_3 = \partial \xi / \partial x_3 = 0$ and the associated stresses are

written at $P=(x_1,h(x_1),x_3)$ as (making use of (5.3)-(5.4) and stress expressions in Sections 2 to 4)

$$\begin{aligned}
\bar{\sigma}_{ii} &= \sigma_{22}^a\delta_{i2} + C_1\frac{(1-p_0^2)\delta_{i1}+(1+3p_0^2)\delta_{i2}}{(1+p_0^2)^2}\int_{-a}^{a}\frac{D_1(x_1')}{x_1-x_1'}dx_1' \\
&\quad + C_1\frac{p_0\left(-(3+p_0^2)\delta_{i1}+(1-p_0^2)\delta_{i2}\right)}{(1+p_0^2)^2}\int_{-a}^{a}\frac{D_2(x_1')}{x_1-x_1'}dx_1' \\
\bar{\sigma}_{i3} &= \sigma_{23}^a\delta_{i2} + C_2\frac{(-p_0\delta_{i1}+\delta_{i2})}{1+p_0^2}\int_{-a}^{a}\frac{D_3(x_1')}{x_1-x_1'}dx_1' \\
\bar{\sigma}_{12} &= \sigma_{12}^a + C_1\frac{(1-p_0^2)}{(1+p_0^2)^2}\int_{-a}^{a}\frac{\left(p_0D_1(x_1')+D_2(x_1')\right)}{x_1-x_1'}dx_1'
\end{aligned} \qquad (5.5)$$

where the subscript i takes the values 1 and 2, $C_1=\mu b/2\pi(1-\nu)$ and $C_2=\mu b/2\pi$; the traction free boundary condition (5.2) then becomes

$$\begin{cases}
\sigma_{22}^a - p_0\sigma_{12}^a + C_1\int_{-a}^{a}\frac{D_1(x_1')}{x_1-x_1'}dx_1' = 0 \\
\sigma_{12}^a + C_1\int_{-a}^{a}\frac{D_2(x_1')}{x_1-x_1'}dx_1' = 0 \\
\sigma_{23}^a + C_2\int_{-a}^{a}\frac{D_3(x_1')}{x_1-x_1'}dx_1' = 0
\end{cases} \qquad (5.6)$$

where the Cauchy principal values of the integrals are to be taken. The type of solution is well known [26]:

$$\begin{aligned}
D_1(x_1) &= \left(1-p_0\frac{\sigma_{12}^a}{\sigma_{22}^a}\right)\frac{\sigma_{22}^a x_1}{\pi C_1\sqrt{a^2-x_1^2}} \equiv \left(1-p_0\frac{\sigma_{12}^a}{\sigma_{22}^a}\right)D_0^{(I)}(x_1) \\
D_2(x_1) &= \frac{\sigma_{12}^a}{\pi C_1}\frac{x_1}{\sqrt{a^2-x_1^2}} \equiv D_0^{(II)}(x_1) \\
D_3(x_1) &= \frac{\sigma_{23}^a}{\pi C_2}\frac{x_1}{\sqrt{a^2-x_1^2}} \equiv D_0^{(III)}(x_1)
\end{aligned}; \qquad (5.7)$$

$D_0^{(i)}$ ($i = I$, *II* and *III* respectively) corresponds to the equilibrium distribution of straight dislocations when the crack is planar in the Ox_1x_3- plane ($p_0 = 0$), extending from $x_1 = -a$ to a, under pure mode i loading. The corresponding relative displacement ϕ_i of the crack faces, in the x_2 ($i = 1$), x_1 ($i = 2$) and x_3 ($i = 3$) directions, are:

$$\begin{aligned}
\phi_1(x_1) &= (1 - p_0\sigma_{12}^a/\sigma_{22}^a)(\sigma_{22}^a b/\pi C_1)(a^2 - x_1^2)^{1/2} \equiv (1 - p_0\sigma_{12}^a/\sigma_{22}^a)\phi_0^{(I)}(x_1), \\
\phi_2(x_1) &= (\sigma_{12}^a b/\pi C_1)(a^2 - x_1^2)^{1/2} \equiv \phi_0^{(II)}(x_1), \\
\phi_3(x_1) &= (\sigma_{23}^a b/\pi C_2)(a^2 - x_1^2)^{1/2} \equiv \phi_0^{(III)}(x_1);
\end{aligned} \tag{5.8}$$

$\phi_0^{(i)}$ ($i = I$, *II* and *III* respectively), similarly as $D_0^{(i)}$, corresponds to the relative displacement of the crack faces when the crack is in Ox_1x_3 under pure mode i loading. D_i is unbounded at $x_1 = \pm a$ and the ϕ_i curve vertical at these end points.

In its general form (5.2) requires a numerical resolution and this is a formidable task; only simple forms of f are tractable. We have given approximate solutions for D_1 and D_3 ($\sigma_{12}^a = 0,\ D_2 = 0$) when $h = 0$ and $\xi = \xi(x_3)$ depends on x_3 only [19]. Fortunately as it appears below, we can reasonably give approximate expressions for the stress about the crack front and crack extension force with f given by (5.1) using D_i (5.7) when the average fracture surface h can be approximated by plane π_0 of ***Figure 2a***.

V-3. Stresses about the crack front

To obtain expressions for the stress about the crack front, we proceed as follows. In the neighbourhood of the crack front located at $x_1 = a$, any point P with coordinates (x_1, x_2, x_3) is characterized by x_2 close to h since the fracture surface is given by $f = h + \xi$ with ξ is small. We can thus consider the Taylor series expansion of $\sigma_{ij}^{(n)}(x_1 - x_1', x_2, x_3)$ (5.4) about $x_2 = h(x_1)$ to first order with respect to $(x_2 - h)$; this gives

$$\sigma_{ij}^{(n)}(x_1 - x_1^{'}, x_2, x_3) = \sigma_{ij}^{(n)}(x_1 - x_1^{'}, h, x_3) + \frac{\partial \sigma_{ij}^{(n)}}{\partial x_2}(x_2 - h) + o(x_2 - h) \tag{5.9}$$

where $o(x_2 - h)$ is the complementary part of the series. Writing $x_1 = a + s$, $0 < s << a$, $\bar{\sigma}_{ij}$ (5.3)-(5.4) is given by the following formula:

$$\bar{\sigma}_{ij}(s, x_2, x_3) = \sum_{n=1}^{3} \int_{a-\delta a}^{a} \sigma_{ij}^{(n)}(a + s - x_1^{'}, x_2, x_3) D_n(x_1^{'}) dx_1^{'} \tag{5.10}$$

with $\delta a << a$. This stress expression means that only those dislocations located about the crack front in x_1-interval $[a - \delta a\ ,\ a]$ will contribute significantly to the stress at $x_1 = a + s$ ahead of the crack tip as *s* tends to zero; any other contribution will be negligible for a sufficiently small value of *s*. We observe that this formula is precise with no place for any other kind of additional stress term. Applying the Taylor expansion (5.9), in $\sigma_{ij}^{(n)}(x_1 - x_1^{'}, h(x_1), x_3)$ and $\partial \sigma_{ij}^{(n)} / \partial x_2$ (in which $x_1 = a + s$), appears the difference ($h(x_1) - h(x_1^{'})$) which we express as follows since x_1 and $x_1^{'}$ (see (5.10)) are close to a: $h(x_1) = h(a) + p(x_1 - a) + o(x_1 - a)$ and $h(x_1^{'}) = h(a) + p(x_1^{'} - a) + o(x_1^{'} - a)$ where $p = \partial h(a) / \partial x_1$; therefore $h(x_1) - h(x_1^{'}) = p(x_1 - x_1^{'}) + o(x_1 - x_1^{'})$. Furthermore in $\bar{\sigma}_{ij}$ (5.10) we restrict ourselves to singularities of the type $s^{-1/2}$ only; this is the singularity that comes into play in the study of planar cracks and gives a well-defined value to the crack extension force. It is sufficient to identify $\sigma_{ij}^{(n)}$ to the unbounded terms with $1/(a + s - x_1')$ in the Taylor expansion (5.9). Assuming $\xi(x_1, x_3)$ and its spatial derivatives with respect to x_3 to be bounded at $x_1 = a$, the involved integrals in (5.10) are of the type $\int D_n(x_1')/(a + s - x_1')dx_1'$ which is calculated approximately taking for D_n the straight edge and screw dislocation distributions (5.7) corresponding to a planar crack π_0 with a straight front parallel to x_3 (***Figure 2a***). We obtain ($\bar{\sigma}_{ij} = \bar{\sigma}_{ij}^{(1)} + \bar{\sigma}_{ij}^{(2)} + \bar{\sigma}_{ij}^{(3)}$ (5.3)):

$$\bar{\sigma}_{ii}^{(1)}(s, x_2, x_3) = \frac{1}{(1 + p^2)^3}\Big([\delta_{i1} + \delta_{i2} + 2\nu\delta_{i3} + (-\delta_{i1} + 3\delta_{i2} + 2\nu\delta_{i3})p^2](1 + p^2)$$

$$+\frac{1}{2}(x_2-h(a))\Big[\delta_{i1}-\delta_{i2}+2(1+\nu)\delta_{i3}-6(\delta_{i1}-\delta_{i2})p^2$$
$$-(-\delta_{i1}+\delta_{i2}+2(1+\nu)\delta_{i3})p^4\Big]\frac{\partial^2\xi}{\partial x_3^2}(a,x_3)\Big)\left(1-p_0\frac{\sigma_{12}^a}{\sigma_{22}^a}\right)\frac{K_I^0}{\sqrt{2\pi}}\frac{1}{\sqrt{s}},$$

$$\bar{\sigma}_{ii}^{(2)}(s,x_2,x_3)=\frac{(-\delta_{i1}+\delta_{i2}-\delta_{i3})p}{(1+p^2)^3}\Bigg([3\delta_{i1}+\delta_{i2}+2\nu\delta_{i3}+(\delta_{i1}-\delta_{i2}+2\nu\delta_{i3})p^2](1+p^2)$$

$$+\frac{1}{2}(x_2-h(a))\Big[3\delta_{i1}+(3+4\nu)\delta_{i2}+2(1+3\nu)\delta_{i3}+(-6\delta_{i1}-2(3-4\nu)\delta_{i2}+8\nu\delta_{i3})p^2$$
$$+(-\delta_{i1}-(1-4\nu)\delta_{i2}-2(1-\nu)\delta_{i3})p^4\Big]\frac{\partial^2\xi}{\partial x_3^2}(a,x_3)\Bigg)\frac{K_{II}^0}{\sqrt{2\pi}}\frac{1}{\sqrt{s}},$$

$$\bar{\sigma}_{ii}^{(3)}(s,x_2,x_3)=\frac{\Big[(p^2-1)\delta_{i1}+\big(1-2\nu-(1+2\nu)p^2\big)\delta_{i2}-2(1+p^2)\delta_{i3}\Big]}{(1-\nu)(1+p^2)^2}\frac{\partial\xi}{\partial x_3}(a,x_3)\frac{K_{III}^0}{\sqrt{2\pi}}\frac{1}{\sqrt{s}}$$

$$\bar{\sigma}_{j3}^{(1)}(s,x_2,x_3)=\frac{p[-(2-\nu)+\nu p^2]\delta_{j1}+[\nu-(2-\nu)p^2]\delta_{j2}}{(1+p^2)^2}\frac{\partial\xi}{\partial x_3}\left(1-p_0\frac{\sigma_{12}^a}{\sigma_{22}^a}\right)\frac{K_I^0}{\sqrt{2\pi}}\frac{1}{\sqrt{s}}$$

$$\bar{\sigma}_{j3}^{(2)}(s,x_2,x_3)=-\frac{[1-(1-\nu)p^2-(2-\nu)p^4]\delta_{j1}+p[1+2\nu-(1-2\nu)p^2]\delta_{j2}}{(1+p^2)^2}\frac{\partial\xi}{\partial x_3}\frac{K_{II}^0}{\sqrt{2\pi}}\frac{1}{\sqrt{s}}$$

$$\bar{\sigma}_{j3}^{(3)}(s,x_2,x_3)=\frac{1}{(1-\nu)(1+p^2)^2}\Bigg((1-\nu)[-p\delta_{j1}+\delta_{j2}](1+p^2)-\frac{1}{2}(x_2-h(a))$$
$$\times\Big[p\big(5-3\nu-(1+\nu)p^2\big)\delta_{j1}-\big(3-\nu-(3-\nu)p^2\big)\delta_{j2}\Big]\frac{\partial^2\xi}{\partial x_3^2}\Bigg)\frac{K_{III}^0}{\sqrt{2\pi}}\frac{1}{\sqrt{s}},$$

$$\bar{\sigma}_{12}^{(1)}(s,x_2,x_3)=\frac{p}{(1+p^2)^3}\Bigg(1-p^4+\frac{1}{2}(x_2-h(a))$$
$$\times\Big[5-2\nu-2(1+2\nu)p^2+(1-2\nu)p^4\Big]\frac{\partial^2\xi}{\partial x_3^2}\Bigg)\left(1-p_0\frac{\sigma_{12}^a}{\sigma_{22}^a}\right)\frac{K_I^0}{\sqrt{2\pi}}\frac{1}{\sqrt{s}},$$

$$\bar{\sigma}_{12}^{(2)}=\frac{1}{(1+p^2)^3}\Bigg(1-p^4+\frac{1}{2}(x_2-h(a))\Big[1+2(13+2\nu)p^2+p^4\Big]\frac{\partial^2\xi}{\partial x_3^2}\Bigg)\frac{K_{II}^0}{\sqrt{2\pi}}\frac{1}{\sqrt{s}},$$

$$\bar{\sigma}_{12}^{(3)}(s,x_2,x_3)=-\frac{p(2-\nu-\nu p^2)}{(1-\nu)(1+p^2)^2}\frac{\partial\xi}{\partial x_3}(a,x_3)\frac{K_{III}^0}{\sqrt{2\pi}}\frac{1}{\sqrt{s}}, \qquad (5.11)$$

where subscript i and j take the values (1, 2 and 3) and (1 and 2) respectively; $p=\partial h(a)/\partial x_1$, K_i^0 ($i=$ I, II and III respectively) is the SIF for the planar crack

in Ox_1x_3 at the origin under pure mode i loading; $K_I^0 = \sigma_{22}^a\sqrt{a\pi}$, $K_{II}^0 = \sigma_{12}^a\sqrt{a\pi}$ and $K_{III}^0 = \sigma_{23}^a\sqrt{a\pi}$. We stress again that s, x_2 and x_3 are arbitrary, $s = x_1 - a << a$ ($s > 0$) and $(x_2 - h(a))$ is small. The parameter p_0 in (5.11) originates from a planar crack π_0 (***Figure 2a***) hypothetically assumed to approximate the average fracture surface $x_2 = h(x_1)$. This suggests that we could write $h(x_1) = p_0x_1 + \Delta h(x_1)$ where Δh is an oscillating function of x_1 taking small positive and negative values. Taking (5.7) for D_n results in coefficients $(1 - p_0\sigma_{12}^a/\sigma_{22}^a)$ and $K_i^0/\sqrt{2\pi s}$ only in (5.11), the other factors have no concern with this approximation.

V-4. Energy considerations

In the following, an expression for the derivative G of the energy of the system with respect to crack area is derived. This serves to discuss the initiation of crack motion. We follow Anongba [19, 20] and the procedure is adapted from Bilby and Eshelby [26].

Allow the right-hand front of the non-planar crack with shape (5.1) (use ***Figure 2c*** to illustrate) to advance (say rigidly for simplicity) from $x_1 = a$ to $a + \delta a$, but apply forces to the freshly formed surfaces to prevent relative displacement; the energy of the system is unaltered. Now allow these forces to relax to zero so that the crack extends effectively from a to $a + \delta a$. The work done by these forces corresponds to a decrease of the energy of the system which we shall estimate (the energy of the system consists of the elastic energy of the medium and the energy of the loading mechanism). The element ds of the fracture surface $x_2 = f(x_1, x_3)$ ahead of the crack front, at a point $P = (x_1, x_2 = f, x_3)$, may be defined by $d\vec{s} = \vec{\gamma}ds$ where $\vec{\gamma}$ is the unit vector perpendicular to ds pointing to the positive x_2- direction. We obtain $d\vec{s} = 1/\sqrt{1 + (\partial f/\partial x_1)^2 + (\partial f/\partial x_3)^2}\,(-\partial f/\partial x_1, 1, -\partial f/\partial x_3)ds$ and take ds to be given as $ds = \sqrt{1 + (\partial f/\partial x_1)^2 + (\partial f/\partial x_3)^2}\,dx_1dx_3$. The component of the force acting on ds in the x_i- direction is $\bar{\sigma}_{ij}ds_j$ (the summation convention on repeated subscripts applies) where $\bar{\sigma}_{ij}$ are stresses ahead of the shorter crack; thus the energy change associated with ds is $\bar{\sigma}_{ij}ds_j\Delta u^{(i)}/2$ (here a summation

is also considered over $i = 1$, 2 and 3) where $\Delta u^{(i)}$ is the difference in displacement across the lengthened crack, just behind its tip, in the $x_i -$ direction. When the crack advances from $x_1 = a$ to $a + \delta a$, the energy decrease associated with a surface element

$$\Delta s = \int_a^{a+\delta a} ds \cong \sqrt{1 + (\partial f / \partial x_1)^2 + (\partial f / \partial x_3)^2}\, \delta a dx_3$$

(δa being small and, when used below, will be let to go to zero) is given as

$$-\delta E = \frac{1}{2} \int_a^{a+\delta a} \sum_i \sum_j \bar{\sigma}_{ij} ds_j \Delta u^{(i)} ,$$

the integration being performed with respect to x_1; we stress that Δs is the sum of the surface elements ds taken at the various points $P = (x_1, x_2 = f, x_3)$ as x_1 only changes from a to $a + \delta a$. Let *G* be a derivative of the energy of the system with respect to crack area. *G* corresponds to the limiting value taken by $-\delta E / \Delta s$ as δa (as also Δs) decreases to zero. Stresses $\bar{\sigma}_{ij}$ generally consist of terms that are either bounded or unbounded as x_1 tends to a; only those stress terms that are singular may contribute a non-zero value to *G*; the bounded terms all contribute nothing. Using (5.11) and defining $\bar{\sigma}^{(i)}(s)$ ($i = 1$, 2 and 3) as

$$\bar{\sigma}^{(i)}(s) \equiv \frac{\delta_{i1} K_{II}^0 + \delta_{i2} K_I^0 + \delta_{i3} K_{III}^0}{\sqrt{2\pi}} \frac{1}{\sqrt{s}} \tag{5.12}$$

we arrive at

$$G(P_0) = \lim_{\delta a \to 0} -\delta E / \Delta s$$
$$= \frac{1}{\sqrt{1 + (\partial f / \partial x_1)^2 + (\partial f / \partial x_3)^2}} \left([\circ] G_0^{(1)} + [\circ\circ] G_0^{(2)} + [\circ\circ\circ] G_0^{(3)} \right) \tag{5.13}$$

where

$$G_0^{(i)} = \lim_{\delta a \to 0} \frac{1}{\delta a} \left(\frac{1}{2} \int_a^{a+\delta a} \bar{\sigma}^{(i)} \Delta u^{(i)} dx_1 \right), \quad i = 1, 2 \text{ and } 3. \tag{5.14}$$

Expressions in $[\circ]$, $[\circ\circ]$ and $[\circ\circ\circ]$ are very long and need not be displayed here; an explicit presentation (5.17) follows. (5.13) gives the value of G at an

arbitrary point $P_0(a, x_2 = f, x_3)$ along the front of the non-planar crack with projected half length a along x_1. The calculation of $\Delta u^{(i)}$ depends on the way the extension of the right-hand front of the crack from $x_1 = a$ to $a + \delta a$ is performed. When $\Delta u^{(i)}$ is obtained from a distribution of dislocations perpendicular to the x_1-direction, we implicitly assume a rigid crack-front displacement. In that case, $\Delta u^{(i)}$ may be obtained from the solution of (5.2) modified to allow for the fact that the crack extends from $x_1 = -a$ to $a + \delta a$ instead of from $-a$ to a. Approximate expressions for $G_0^{(i)}$ ($i = 1$, 2 and 3) correspond to a planar distribution of straight edge and screw dislocations. When the crack has the geometry of ***Figure 2a*** with $\theta_0 = 0$ ($p_0 = 0$), Bilby and Eshelby [26] have shown that $G_0^{(1)} = K_{II}^{0\,2}(1-\nu^2)/E \equiv G_0^{II}$, $G_0^{(2)} = K_I^{0\,2}(1-\nu^2)/E \equiv G_0^I$ and $G_0^{(3)} = K_{III}^{0\,2}(1+\nu)/E \equiv G_0^{III}$ where E is Young's modulus. The corresponding dislocation distributions are $D_0^{(II)}$, $D_0^{(I)}$ and $D_0^{(III)}$ (see (5.7)) with associated relative displacements of the faces of the crack $\phi_0^{(II)}$, $\phi_0^{(I)}$ and $\phi_0^{(III)}$ (5.8). In the same approximation and using the dislocation distributions D_i (5.7) corresponding to a planar crack π_0 (***Figure 2a***) inclined by θ_0 (about axis Ox_3) with respect to Ox_1x_3, we arrive at

$$\begin{aligned} G_0^{(1)} &= G_0^{II}, \\ G_0^{(2)} &= \left(1 - p_0 \frac{\sigma_{12}^a}{\sigma_{22}^a}\right) G_0^I, \\ G_0^{(3)} &= G_0^{III}. \end{aligned} \tag{5.15}$$

Adopting approximation (5.15) and defining $\tilde{G}(P_0)$ as $\tilde{G}(P_0) = G(P_0)/(G_0^I + G_0^{II} + G_0^{III})$, we obtain (with $M_{12} \equiv \sigma_{12}^a/\sigma_{22}^a$, $M_{13} \equiv \sigma_{23}^a/\sigma_{22}^a$, $M_{23} \equiv \sigma_{23}^a/\sigma_{12}^a$)

$$\tilde{G}(P_0) = \sum_{i,j=1}^{3} \tilde{G}_j^{(i)}(P_0) \tag{5.16}$$

where

$$\tilde{G}_1^{(1)} = -\frac{1}{2(1+p^2)^3}\frac{\partial f(a,x_3)/\partial x_1}{\sqrt{1+(\partial f/\partial x_1)^2+(\partial f/\partial x_3)^2}}\Bigg(2(1-p^4)-2(1+p^2)\Big[p_0(1-p^2)$$
$$+p(3+p^2)\Big]M_{12}-\frac{2}{1-\nu}(1-p^4)M_{13}\frac{\partial\xi}{\partial x_3}+\Big[1-6p^2+p^4-\Big(p_0(1-6p^2+p^4)$$
$$+p(3-6p^2-p^4)\Big)M_{12}\Big]\xi\frac{\partial^2\xi}{\partial x_3^2}\Bigg)\frac{(1-\nu)M_{12}}{\Big[1-\nu+(1-\nu)M_{12}^2+M_{13}^2\Big]},$$

$$\tilde{G}_2^{(1)} = \frac{1}{2(1+p^2)^3}\frac{1}{\sqrt{1+(\partial f/\partial x_1)^2+(\partial f/\partial x_3)^2}}\Bigg(2p(1-p^4)+2(1-p^4)(1-p_0p)M_{12}$$
$$-\frac{2}{1-\nu}p(1+p^2)(2-\nu-\nu p^2)M_{13}\frac{\partial\xi}{\partial x_3}+\Big[p\Big(5-2\nu-2(1+2\nu)p^2+(1-2\nu)p^4\Big)$$
$$+\Big(1+2(13+2\nu)p^2+p^4-p_0p\Big(5-2\nu-2(1+2\nu)p^2+(1-2\nu)p^4\Big)\Big)M_{12}\Big]$$
$$\times\xi\frac{\partial^2\xi}{\partial x_3^2}\Bigg)\frac{(1-\nu)M_{12}}{\Big[1-\nu+(1-\nu)M_{12}^2+M_{13}^2\Big]},$$

$$\tilde{G}_3^{(1)} = -\frac{1}{(1+p^2)^2}\frac{\partial f/\partial x_3}{\sqrt{1+(\partial f/\partial x_1)^2+(\partial f/\partial x_3)^2}}\Bigg(-p(1+p^2)M_{13}+\Big[p\Big(-2+\nu+\nu p^2\Big)$$
$$-\Big(1-(1-\nu)p^2-(2-\nu)p^4+p_0p(-2+\nu+\nu p^2)\Big)M_{12}\Big]\frac{\partial\xi}{\partial x_3}-p\Big(5-3\nu-(1+\nu)p^2\Big)\frac{M_{13}}{2(1-\nu)}$$
$$\times\xi\frac{\partial^2\xi}{\partial x_3^2}\Bigg)\frac{(1-\nu)M_{12}}{\Big[1-\nu+(1-\nu)M_{12}^2+M_{13}^2\Big]},$$

$$\tilde{G}_1^{(2)} = -\frac{1}{2(1+p^2)^3}\frac{\partial f/\partial x_1}{\sqrt{1+(\partial f/\partial x_1)^2+(\partial f/\partial x_3)^2}}\Bigg(2p(1-p^4)+2(1-p^4)(1-p_0p)M_{12}$$
$$-\frac{2}{1-\nu}p(1+p^2)(2-\nu-\nu p^2)M_{13}\frac{\partial\xi}{\partial x_3}+\Big[p\Big(5-2\nu-2(1+2\nu)p^2+(1-2\nu)p^4\Big)$$
$$+\Big(1+2(13+2\nu)p^2+p^4-p_0p\Big(5-2\nu-2(1+2\nu)p^2+(1-2\nu)p^4\Big)\Big)M_{12}\Big]$$

$$\times\xi\frac{\partial^2\xi}{\partial x_3^2}\Big)\frac{(1-\nu)(1-p_0M_{12})}{\left[1-\nu+(1-\nu)M_{12}^2+M_{13}^2\right]},$$

$$\tilde{G}_2^{(2)}=\frac{1}{2(1+p^2)^3}\frac{1}{\sqrt{1+(\partial f/\partial x_1)^2+(\partial f/\partial x_3)^2}}\Big(2(1+p^2)(1+3p^2)-2(1+p^2)\Big(p_0(1+3p^2)$$

$$-p(1-p^2)\Big)M_{12}+\frac{2}{1-\nu}(1+p^2)(1-2\nu-(1+2\nu)p^2)M_{13}\frac{\partial\xi}{\partial x_3}+\Big[-1+6p^2-p^4$$
$$+\Big(p_0(1-6p^2+p^4)+p\Big(3+4\nu-2(3-4\nu)p^2-(1-4\nu)p^4\Big)\Big)M_{12}\Big]$$

$$\times\xi\frac{\partial^2\xi}{\partial x_3^2}\Big)\frac{(1-\nu)(1-p_0M_{12})}{\left[1-\nu+(1-\nu)M_{12}^2+M_{13}^2\right]},$$

$$\tilde{G}_3^{(2)}=-\frac{1}{(1+p^2)^2}\frac{\partial f/\partial x_3}{\sqrt{1+(\partial f/\partial x_1)^2+(\partial f/\partial x_3)^2}}\Big((1+p^2)M_{13}+\Big[\nu-(2-\nu)p^2$$

$$-\Big(p_0(\nu-(2-\nu)p^2)+p(1+2\nu-(1-2\nu)p^2)\Big)M_{12}\Big]\frac{\partial\xi}{\partial x_3}+\frac{1}{2(1-\nu)}\Big(3-\nu-(3-\nu)p^2\Big)M_{13}$$

$$\times\xi\frac{\partial^2\xi}{\partial x_3^2}\Big)\frac{(1-\nu)(1-p_0M_{12})}{\left[1-\nu+(1-\nu)M_{12}^2+M_{13}^2\right]},$$

$$\tilde{G}_1^{(3)}=-\frac{1}{(1+p^2)^2}\frac{\partial f/\partial x_1}{\sqrt{1+(\partial f/\partial x_1)^2+(\partial f/\partial x_3)^2}}\Big(-p(1+p^2)M_{13}^2-\Big[p(2-\nu-\nu p^2)M_{13}$$

$$+\Big(1-(1-\nu)p^2-p_0p(2-\nu-\nu p^2)-(2-\nu)p^4\Big)M_{12}M_{13}\Big]\frac{\partial\xi}{\partial x_3}-\frac{p\Big(5-3\nu-(1+\nu)p^2\Big)}{2(1-\nu)}$$
$$\times M_{13}^2\xi\frac{\partial^2\xi}{\partial x_3^2}\Big)\frac{1}{\left[1-\nu+(1-\nu)M_{12}^2+M_{13}^2\right]},$$

$$\tilde{G}_2^{(3)}=\frac{1}{(1+p^2)^2}\frac{1}{\sqrt{1+(\partial f/\partial x_1)^2+(\partial f/\partial x_3)^2}}\Big((1+p^2)M_{13}^2+\Big[(\nu-(2-\nu)p^2)M_{13}$$

$$-\Big(p_0(\nu-(2-\nu)p^2)+p(1+2\nu-(1-2\nu)p^2)\Big)M_{12}M_{13}\Big]\frac{\partial\xi}{\partial x_3}+\frac{\Big(3-\nu-(3-\nu)p^2\Big)}{2(1-\nu)}$$

$$\times M_{13}^2 \xi \frac{\partial^2 \xi}{\partial x_3^2}\Bigg)\Big[1-\nu+(1-\nu)M_{12}^2+M_{13}^2\Big],$$

$$\tilde{G}_3^{(3)} = -\frac{1}{2(1+p^2)^3}\frac{\partial f/\partial x_3}{\sqrt{1+(\partial f/\partial x_1)^2+(\partial f/\partial x_3)^2}}\Bigg(4\nu(1+p^2)^2\big[M_{13}-(p+p_0)M_{12}M_{13}\big]$$

$$-\frac{4}{1-\nu}(1+p^2)^2 M_{13}^2\frac{\partial \xi}{\partial x_3}+\Big[2(1+\nu)(1-p^4)M_{13}-\Big(2(1+\nu)p_0(1-p^4)$$

$$+p\Big(2(1+3\nu)+8\nu p^2-2(1-\nu)p^4\Big)\Big)M_{12}M_{13}\Big]\xi\frac{\partial^2 \xi}{\partial x_3^2}\Bigg)\Big[1-\nu+(1-\nu)M_{12}^2+M_{13}^2\Big], \qquad (5.17)$$

For the planar crack with a straight front, the decrease of the energy of the system ($-\delta E$), divided by the surface element $dl\delta a$ (l runs along the crack front), is defined as the crack extension force per unit edge length of the crack front (see [26] for example). In the present study, we shall refer to G (5.13) as the crack extension force per unit length of the crack front. In Section 6 we give a more detailed description of G for special cracks as illustrated in ***Figure2***.

VI – SPECIAL CRACKS

VI-1. Cracks with a straight front

We consider first the crack in ***Figure 2b***; it extends from $x_1=-a$ to a and runs indefinitely in the x_3- direction. The crack front is straight parallel to x_3 ($\xi=0$) and $f=h(x_1)$ independent of x_3. We assume the crack to fluctuate about plane π_0 (***Figure 2a***) and take D_i (5.7) as the distribution of the equilibrium crack dislocations. Under such conditions the reduced crack extension force $\tilde{G}$ (5.16)-(5.17) under mixed mode I+II+III loading takes the form

$$\tilde{G}(P_0)=\frac{1}{\sqrt{1+p^2}}\frac{1-2p_0M_{12}+(1+p_0^2)M_{12}^2+M_{13}^2/(1-\nu)}{1+M_{12}^2+M_{13}^2/(1-\nu)} \qquad (\xi=0;h=h(x_1)) \quad (6.1)$$

at point $P_0(a,x_2=h(a),x_3)$ of the crack front located at $x_1=a$; $p=\partial h(a)/\partial x_1=\tan\theta$ (for θ, see ***Figure 2b***).

The second crack we present is given in ***Figure 2a***. This is a tilted planar crack corresponding to the rotation of plane Ox_1x_3 about $0x_3$ by angle $\theta_0 = \tan^{-1}(p_0)$. The crack front is straight ($\xi = 0$) and $h = p_0 x_1$. The normalized crack extension force $\tilde{G}$ (5.16)-(5.17) then reads

$$\tilde{G}(P_0) = \frac{1}{\sqrt{1+p_0^2}} \frac{1 - 2p_0 M_{12} + (1+p_0^2)M_{12}^2 + M_{13}^2/(1-\nu)}{1 + M_{12}^2 + M_{13}^2/(1-\nu)} \qquad (\xi=0; h=p_0 x_1) \qquad (6.2)$$

at point $P_0(a, x_2 = p_0 a, x_3)$ of the crack front located at $x_1 = a$. ***Figure 3*** is a plot of $\tilde{G}$ (6.2) as a function of θ_0 for different M_{12} values when $M_{13} = 0$ (mixed mode I+II loading). We expect that for a tilted plane crack π_0 (***Figure 2a***) to be observable experimentally, it is necessary that $\tilde{G}$ be larger than 1. As we can see from ***Figure 3***, this occurs for sufficiently large M_{12} and θ_0 values; the larger the M_{12} (dominant mode II loading) the smaller the θ_0 values for which $\tilde{G} > 1$. When M_{12} is very large and $M_{13} = 0$ (pure mode II loading), $\tilde{G}(P_0) \cong 1/\cos\theta_0$ increases continually with θ_0 from the value 1 ($\theta_0 = 0$); this reveals the importance of mode II loading in increasing $\tilde{G}$. The result $\tilde{G} > 1$ under certain conditions (***Figure 3***) agrees with experiments showing that when a mode II loading (in addition to mode I) is applied to a planar crack located in Ox_1x_3, the subsequent fracture propagation path departs from x_1x_3 ([16, 17]; see also [5] for additional references). Under mixed mode I+III loading ($M_{12} = 0$) $\tilde{G}(P_0) \cong \cos\theta_0$ (independent of M_{13}) decreases continually with θ_0 from the value 1 ($\theta_0 = 0$); adding mode III to mode I loading contributes nothing to the initiation of π_0 motion.

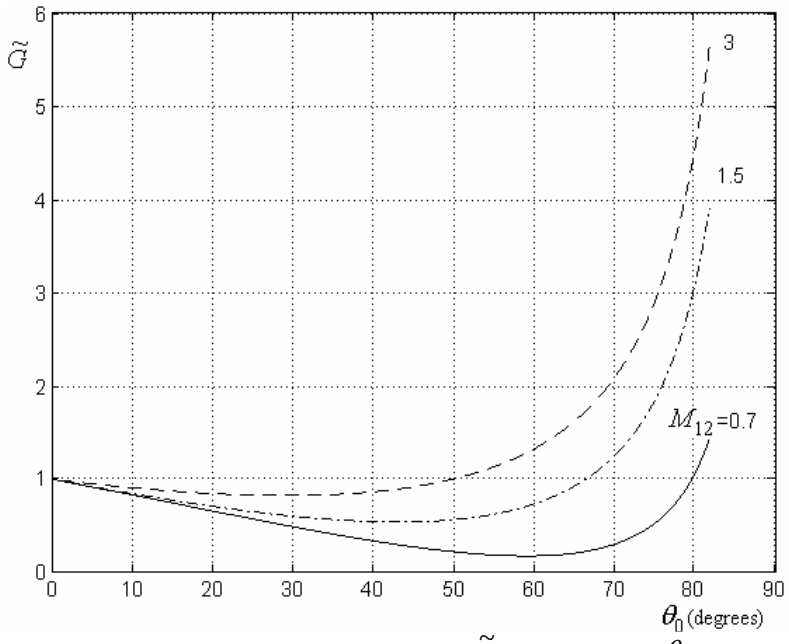

Figure 3: *Normalized crack extension force* $\tilde{G}$ *(6.2) versus* θ_0 *for a planar crack* π_0 *with a straight front parallel to* Ox_3 *(**Figure 2a**), tilted about* Ox_3 *by an angle* $\theta_0 = \tan^{-1} p_0$ *from* Ox_1x_3*, under mixed mode I+II loading (*$M_{13} = 0$*). The curves correspond from bottom to top to* $M_{12} = 0.7$*, 1.5 and 3.*

VI-2. Cracks with a non-straight front

The last example we shall describe is a non-planar crack (***Figure2c***) with a segmented front (***Figure 2d***) whose average fracture surface is plane π_0 tilted about Ox_3 by angle θ_0 from Ox_1x_3. The crack front at $x_1 = a$ runs indefinitely in the x_3- direction and is located in a x_2x_3- plane. We describe ξ below taking locally B as origin as in ***Figure 2d***. ξ is then odd and $(2\lambda = \lambda_A + \lambda_B)-$ periodical with respect to x_3 where λ_A and λ_B (***Figure 2d***) are the projected length along x_3 of planar facet A and B respectively. ξ is given over a wavelength as

$$\begin{aligned} \xi &= \tan\phi_B x_3, && |x_3| \le \lambda_B/2 \\ &= \tan\phi_A(-x_3 + \lambda), && x_3 \in [\lambda_B/2,\ \lambda_B/2 + \lambda_A]. \end{aligned} \tag{6.3}$$

We assume general loading (mixed mode I+II+III), write $p_0 = p = \tan\theta$ for simplicity in (5.16)-(5.17) for the reduced crack extension force, now denoted $\tilde{G}_v$, and express the spatial average $<\tilde{G}_v>$ of $\tilde{G}_v$ defined as $<\tilde{G}_v> = (1/2\lambda)\int_0^{2\lambda} \tilde{G}_v dx_3$. We obtain

$$<\tilde{G}_v> = \frac{1}{(1+p^2)^2}\Big\{(1-\nu)(1+p^2)^2\Big[1-2pM_{12}+(1+p^2)M_{12}^2+M_{13}^2/(1-\nu)\Big]v_0$$

$$+\Big[-2\nu(1+p^2)^2 M_{13}+p\big(2\nu+5\nu p^2-(2-3\nu)p^4\big)M_{12}M_{13}\Big]v_1+\Big[-(1-\nu)\big(\nu-(2-\nu)p^2\big)$$
$$+(1-\nu)p\big(3+3\nu-(5-3\nu)p^2\big)M_{12}+(1-\nu)\big(1-(4+\nu)p^2+(1-\nu)p^4\big)M_{12}^2$$
$$+2(1+p^2)M_{13}^2/(1-\nu)\Big]v_2\Big\}\frac{1}{\Big[1-\nu+(1-\nu)M_{12}^2+M_{13}^2\Big]} \qquad (6.4)$$

where

$$v_0 = \big(1/(p_A+p_B)\big)\Big(p_A/\sqrt{1+p^2+p_B^2}+p_B/\sqrt{1+p^2+p_A^2}\Big),$$
$$v_1 = \big(p_A p_B/(p_A+p_B)\big)\Big(-1/\sqrt{1+p^2+p_A^2}+1/\sqrt{1+p^2+p_B^2}\Big),$$
$$v_2 = \big(p_A p_B/(p_A+p_B)\big)\Big(p_A/\sqrt{1+p^2+p_A^2}+p_B/\sqrt{1+p^2+p_B^2}\Big) \qquad (6.5)$$

and $p_A = \tan\phi_A$, $p_B = \tan\phi_B$. Hence $<\tilde{G}_v>$ is a function of parameters $(p, p_A, p_B; M_{12}, M_{13})$. When ϕ_B (or ϕ_A) equals zero, the crack front is essentially straight parallel to the x_3 – direction. The corresponding crack is similar to planar crack π_0 (***Figure 2a***); under such conditions $<\tilde{G}_v>$ (6.4) is identical to (6.2).

We first focus on the effect of M_{12} (mode II loading) when $\phi_B \neq 0$. In absence of mode III ($M_{13} = 0$) and $p = 0$, (6.4) becomes under such conditions $<\tilde{G}_v>$ increases with M_{12} from the value $(v_0 - w_2)$ ($M_{12} = 0$, pure mode I loading) to $(v_0 + v_2)$ (M_{12} very large, pure mode II loading). We note from expression (5.11) of the stress about the crack front (when $p = 0$) that under pure mode I loading the $<\tilde{G}_v>$ term v_0 originates from $\bar{\sigma}_{22}$ and the term

$(-\nu_2)$ from $\bar{\sigma}_{23}$ whereas under pure mode II the $<\tilde{G}_v>$ term ν_0 originates from $\bar{\sigma}_{12}$ and the term ν_2 from $\bar{\sigma}_{13}$. We have reported on ***Figure 4*** $<\tilde{G}_v>$ (6.4) as a function of (θ,ϕ_A) for constant $\phi_B = 70°$, $M_{13} = 0$ and M_{12} equal to ((a) 0.1, (b) 0.5, (c) 1 and (d) 2). (θ,ϕ_A) regions where $<\tilde{G}_v>$ is larger than 1 grow as M_{12} increases indicating that mode II loading contributes to improve the condition for the motion initiation of a crack whose fronts consist of straight segments. A similar behaviour as in ***Figure 4*** is observed when $M_{13} \neq 0$, other conditions remaining unchanged. When $p \neq 0$ it can be noted that a term with the product $M_{12}M_{13}$ exists in $<\tilde{G}_v>$ (6.4) indicating a correlated effect between modes II and III.

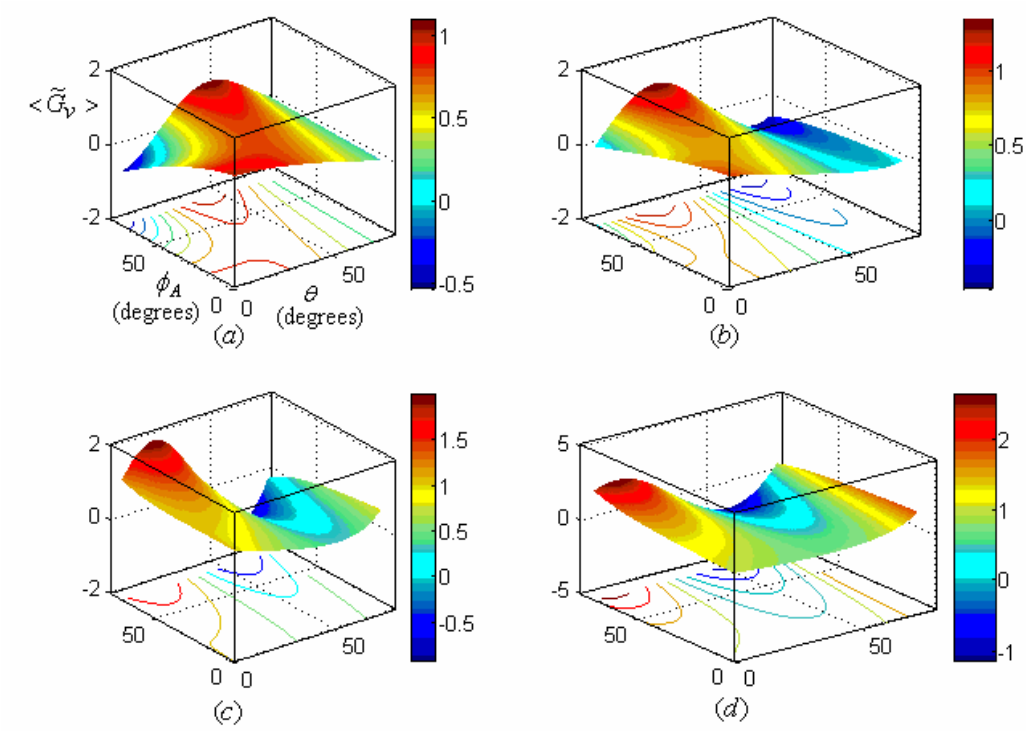

Figure 4: *Surfaces* $<\tilde{G}_v>(\theta,\phi_A)$ *with associated contours at constant* $\phi_B = 70°$, $M_{13} = 0$ *and four different* M_{12}*: (a)* $M_{12} = 0.1$*, (b) 0.5, (c) 1 and (d) 2 (see text).* $\nu = 1/3$.

$$<\tilde{G}_v> = \nu_0 + \nu_2\left(M_{12}^2 - \nu\right)/\left(M_{12}^2 + 1\right) \quad (p = 0; M_{13} = 0); \tag{6.6}$$

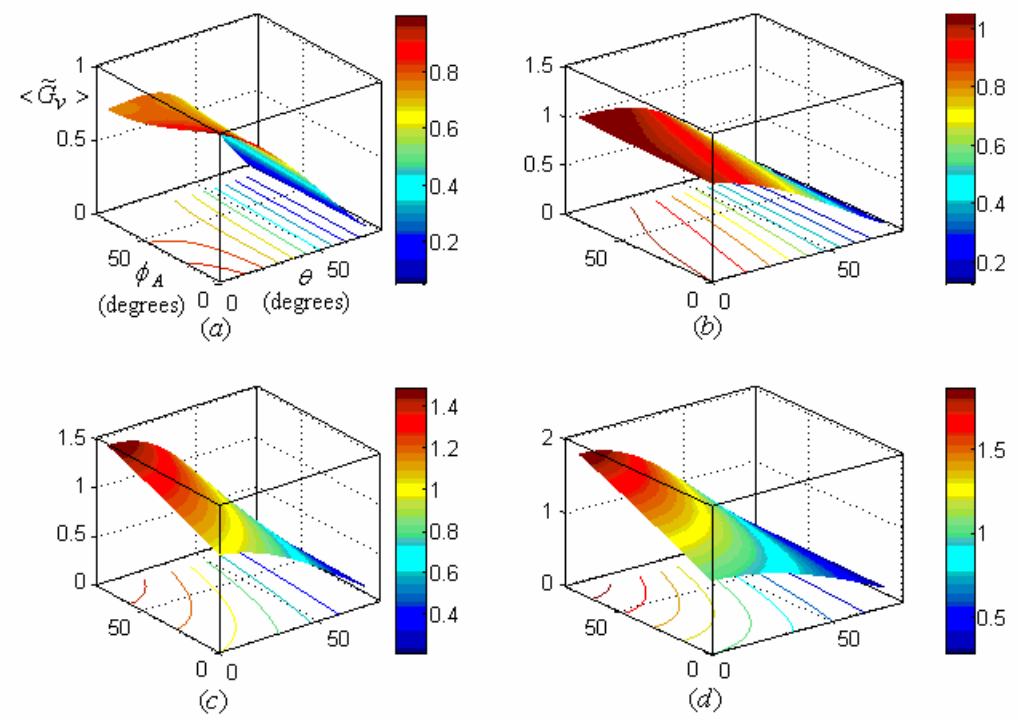

Figure 5: *Surfaces* $<\tilde{G}_v>(\theta,\phi_A)$ *with associated contours at constant* $\phi_B = 20°$, $M_{12} = 0.2$ *and four different* M_{13}*: (a)* $M_{13} = 0.1$*, (b) 0.5, (c) 1 and (d) 2 (see text).* $\nu = 1/3$.

In absence of mode II ($M_{12} = 0$) and $p = 0$, (6.4) becomes ($\phi_B \neq 0$)

$$<\tilde{G}_v> = v_0 - v_1 \frac{2\nu M_{13}}{1-\nu+M_{13}^2} + v_2 \frac{2M_{13}^2 - \nu(1-\nu)^2}{(1-\nu)(1-\nu+M_{13}^2)} \quad (p=0; M_{12}=0). \qquad (6.7)$$

This case is considered in some details elsewhere [19]: conditions under which $<\tilde{G}_v>$ (6.7) is maximum are established; these conditions are then confronted with experimental measurements of crack-front twist angle versus applied stress M_{13} and found to conform to situations where non-planar cracks are favourably observed [19]. $<\tilde{G}_v>$ (6.7) increases with M_{13} from the value $(v_0 - v_2)$ ($M_{13} = 0$ pure mode I loading) to $(v_0 + (2/1-\nu)v_2)$ (M_{13} very large, pure mode III loading); for the latter value the term v_0 originates

from $\bar{\sigma}_{23}$ and the term $(2/1-\nu)\nu_2$ from $\bar{\sigma}_{33}$. We note that the value $(\nu_0+(2/1-\nu)\nu_2)$ reached by $<\tilde{G}_\nu>$ ($p=0$) under pure mode III loading is appreciably larger than the corresponding value $(\nu_0+\nu_2)$ obtained above under pure mode II. This reveals (see also below ***Figures 5*** and ***6***) a stronger effect of mode III loading (as compared to mode II) superimposed over mode I for improving the conditions for non-planar crack motion.

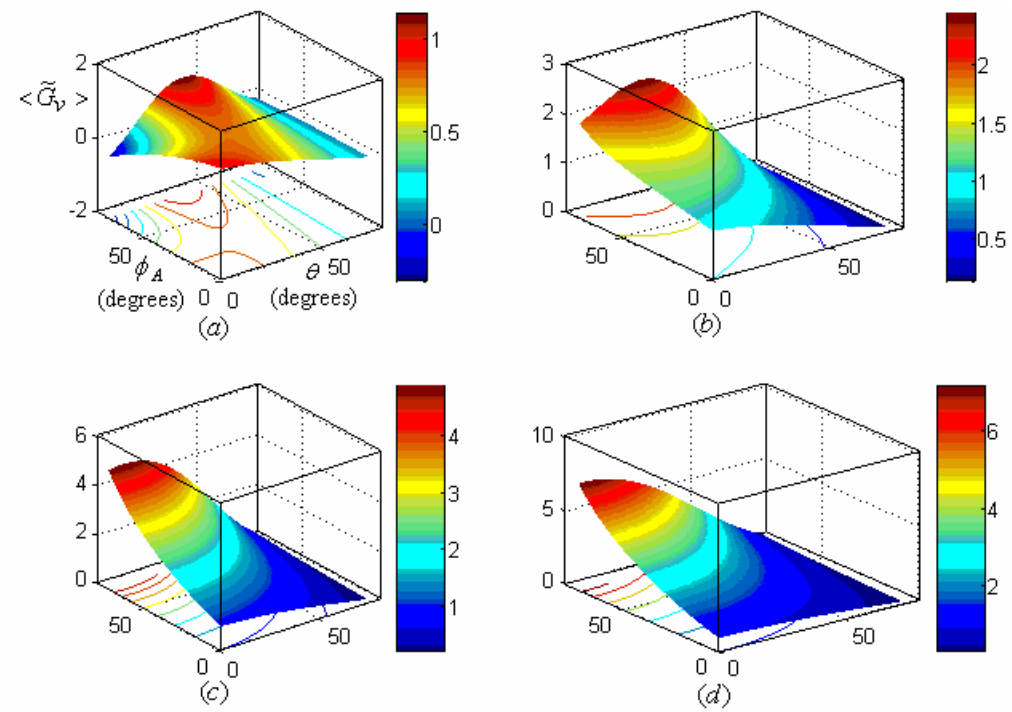

Figure 6: $<\tilde{G}_\nu>(\theta,\phi_A)$ *with similar conditions as in* ***Figure 5*** *except* $\phi_B=70°$ *:* $M_{12}=0.2$, $\nu=1/3$ *and* M_{13} *in (a), (b), (c) and (d) as in* ***Figure5****.*

Figure 5 displays $<\tilde{G}_\nu>$ (6.4) as a function of (θ,ϕ_A) for constant $\phi_B=20°$, $M_{12}=0.2$ and for different values of M_{13} ((a) 0.1, (b) 0.5, (c) 1 and (d) 2). $<\tilde{G}_\nu>$ is larger than 1 for sufficiently large M_{13} with corresponding (θ,ϕ_A) area increasing with M_{13}, ***Figure 5b*** to ***d***; under such conditions $<\tilde{G}_\nu>$ increases with ϕ_A (see ***Figure 5c*** and ***d*** for instance). Hence the more the crack front departs locally from the average straight line, the larger the $<\tilde{G}_\nu>$. This behaviour is amplified when we take $\phi_B=70°$, ***Figure 6***, other

conditions remaining similar. It thus appears that mode III loading superimposed over mode I promotes crack front segmentation. This is in full agreement with experiments ([4 to 7], among others).

VII – CONCLUDING REMARKS

The method of analysis in the present study consists in using explicit expressions of the stress field of dislocations to give an estimated value to the crack-tip stress and crack extension force. More precisely, we are dealing with three types of dislocation with a sinusoidal shape (edges I and II and screws) because from the expression of the displacement and stress fields of a sinusoidal dislocation, one can derive that of a dislocation with the more general form (2.1) (Section 2.2; [19]). One can distinguish the sinusoidal edge I dislocation [23]: this is a dislocation located at the origin (Burgers vector $(0,b,0)$), extending indefinitely in the x_3- direction, whose shape is given by an equation of the type $x_2 = \xi_0 \sin \kappa_0 x_3$ spreading in the Ox_2x_3- plane; the sinusoidal edge II and screw dislocations have the same characteristics except Burgers vectors $(b,0,0)$ and $(0,0,b)$ in x_1 and x_3 directions, respectively.

The expression of the stress at the crack tip is the sum of three terms (5.11) associated with the three types of dislocation. (5.11) is valid under ξ small only, the shape of ξ being arbitrary, with the meaning that there is no restriction on the spatial derivatives of ξ ($\partial\xi/\partial x_3$ and $\partial^2\xi/\partial x_3^2$, for instance) with regard to edges I and screws. Indeed the displacement and stress fields of edges I and screws (namely (2.14)(2.16) and (4.2)(4.4)) are established from a linear form with respect to ξ ((2.2) and (4.1)) of plastic distortions β_{12}^* and β_{13}^* (note that the exact relation is $\beta_{12}^*(\vec{x}) = b\delta(x_1)H(x_2 - f) = \beta_{13}^*(\vec{x})$). Relations (2.2) and (4.1) are valid under the condition ξ small only, the shape of ξ being arbitrary. Use is then made of formula (5.10) to give an expression to the stress at the crack tip. No additional hypothesis on ξ and its spatial derivatives are introduced indicating that the final result (5.11) is valid under condition ξ small only. With regard to edges II, the exact form of the plastic distortion is given by (3.2) whereas we have used the approximate expression $\beta_{21}^*(\vec{x}) = b\delta(x_2 - \xi_n \sin \kappa_n x_3)H(-x_1)$; this means that we assume small the spatial derivative $\partial\xi/\partial x_3$. Consequently

$\bar{\sigma}_{ij}^{(2)}$ in (5.11) is valid under the condition ξ and its spatial derivatives $\partial\xi/\partial x_3$ and $\partial^2\xi/\partial x_3^2$ small. When calculating the crack extension force G (5.13) or $\tilde{G}$ (5.16)-(5.17), the terms with $(x_2 - h(a))\partial^2\xi/\partial x_3^2$ in $\bar{\sigma}_{ij}^{(2)}$ ($\bar{\sigma}_{ii}^{(2)}$ and $\bar{\sigma}_{12}^{(2)}$ (5.11) for instance) contribute in terms with $\xi\partial^2\xi/\partial x_3^2$ in G; the factor $\xi\partial^2\xi/\partial x_3^2$ is of second order and as so should be discarded with regard to edges II only (this factor is admissible for the other dislocation types, edges I and screws). We note that (5.17) for the reduced crack extension force $\tilde{G}$ contains any term with $\xi\partial^2\xi/\partial x_3^2$ originating from $\bar{\sigma}_{ij}^{(m)}$ ($m=1$, 2 and 3) (5.11). However we stress that terms with $\xi\partial^2\xi/\partial x_3^2$ are not present in (6.4) because $\partial^2\xi/\partial x_3^2 = 0$ for the special crack discussed in Section 6.2. Equally, they are not present when the crack front is straight ($\xi \equiv 0$), Section 6.1.

A question arises: what may be the implication, with regard to the precision of our $\tilde{G}$ result (5.16)-(5.17), of a more restrictive condition on the shape of ξ suffered by the edges II? The shape of ξ (smooth or rough) plays an important role in the analysis of the segmentation process of the crack front [19]: when the crack front is smooth (ξ and $\partial\xi/\partial x_3$ small) $<\tilde{G}>=1$ and no comparison with experiment is possible via $<\tilde{G}>$; however when the crack front is rough (ξ small only, no limitation on the value of $\partial\xi/\partial x_3$), $<\tilde{G}>$ may be express as a function of the crack front characteristic parameters and applied loadings, and a comparison with experiment is then possible [19]. Experimentally this is the mode III loading that plays a preponderant role on the segmentation process of the crack front (Section 1). The mode II loading to which is attached the edges II plays a minor role. Consequently our result (5.16)-(5.17) should retain its precision with regard to experiment. The behaviours of $\tilde{G}$ (6.2) and $<\tilde{G}>$ (6.4) presented in Section 6 for special cracks agree with experiments. We have identified crack configurations for which $\tilde{G}$ and $<\tilde{G}>$ are larger than 1 (the value 1 corresponds to a planar crack in Ox_1x_3); these corroborate the fact that non planar cracks fluctuating about an average fracture plane π_0 (***Figure 2***) are observed experimentally.

In conclusion, a model of non-planar crack of finite length under mixed mode I+II+III loading, fluctuating about an average fracture surface $h = h(x_1)$ that departs from Ox_1x_3, has been investigated. The crack

front has an arbitrary shape f spreading in x_2x_3 planes. We have established expressions for both the stress about the crack front (5.11) and the crack extension force *G* per unit length of the crack front (5.13) (5.16). We have averaged *G* over x_3 for one special crack with a segmented front and found crack configurations for which the average crack extension force $< G >$ is larger than the value corresponding to that of the planar crack in Ox_1x_3 under mixed mode I+II+III loading thus confirming the occurrence of non-planar fracture observed in real materials.

REFERENCES

[1]- H.D. BUI, "Mécanique de la rupture", Ed. Masson, Paris (1978)

[2]- B.R. LAWN, "Fracture of brittle solids", Ed. Cambridge University Press, Cambridge (1993)

[3]- K.B. BROBERG, "Cracks and Fracture", Ed. Academic Press, London (1999)

[4]- E. SOMMER, Eng. Fract. Mecha., 1 (1969) 539 - 546

[5]- M.L. COOKE and D.D. POLLARD, *J. Geophys. Res.*, 101 (1996) 3387 – 3400

[6]- J.R. YATES and K.J. MILLER, *Fatigue Fract. Eng. Mater. Struct.*, 12 (1989) 259 - 270

[7]- F. HOURLIER and A. PINEAU, Mém. Sci. Rev. Métall., 76 (1979) 175 – 185

[8]- T.M. MACCAGNO and J.F. KNOTT, Eng. Fract. Mech., 34 (1989) 65 – 86

[9]- R.V. MAHAJAN and K. RAVI-CHANDAR, *Int. J. Fract*., 41 (1989) 235 – 252

[10]- A.L. THOMAS and D.D. POLLARD, *J. Struct. Geol.*, 15 (1993) 323 – 334

[11]- Y. UEDA, K. IKEDA, T. YAO and M. AOKI, *Eng. Fract. Mech.*, 18 (1983) 1131-1158

[12]- H. GAO, *ASME J. Appl. Mech*., 59 (1992) 335 - 343

[13]- G. XU, A.F. BOWER and M. ORTIZ, *Int. J. Solids Struct*., 31 (1994) 2167 - 2193

[14]- [[14] - R.C. BALL and H. LARRALDE, *Int. J. Fract*., 71 (1995) 365 - 377

[15]- A.B. MOVCHAN, H. GAO and J.R. WILLIS, *Int. J. Solids Struct*., 35 (1998) 3419 - 3453

[16]- F. ERDOGAN and G.C. SIH, *Trans. Am. Soc. Mech. Engng*., 85 (1963) 519 - 527

[17]- C.C. RADON, P.S. LEVER and L.E. CULVER, In: "Fracture", Ed. *UW Press*, Vol 3 (1977) 1113 – 1118

[18]- V. LAZARUS, J.-B. LEBLOND and S.-E. MOUCHRIF, *J. Mech. Phys. Sol*., 49 (2001) 1399 – 1420, Ibid., 1421 – 1443
[19]- P.N.B. ANONGBA, *Rev. Ivoir. Sci. Technol.*, 14 (2009) 55 - 86
[20]- P.N.B. ANONGBA, *Physica Stat. Sol. B*, 194 (1996) 443 - 452
[21]- [P.N.B. ANONGBA, *Int. J. Fract*., 124 (2003) 17 - 31
[22]- P.N.B. ANONGBA and V. VITEK, *Int. J. Fract*., 124 (2003) 1 - 15
[23]- P.N.B. ANONGBA, *Physica Stat. Sol. B*, 190 (1995) 135 - 149
[24]- T. MURA, *Adv. Mater. Research*, 3 (1968) 1 – 108
[25]- T. MURA, "Micromechanics of defects in solids", Ed. Martinus Nijhoff Publishers, Dordrecht (1987)
[26]- B.A. BILBY and J.D. ESHELBY, In: "Fracture", Ed. *Academic Press (H. Liebowitz), New York*, Vol 1 (1968) 99 – 182